Electronic Supplementary Material (ESI) for Chemical Communications.
This journal is © The Royal Society of Chemistry 2019

Electronic Supporting Information

Versatile, one-pot introduction of nonahalogenated 2-ammonio-decaborate ions as boron cluster scaffolds into organic molecules; host-guest complexation with γ-cyclodextrin

Suzan El Anwar,[a] Khaleel Assaf,[b,c] Barbara Begaj,[b] Zdeňka Růžičková,[d] Maksim A. Samsonov,[d] Josef Holub,[a] Dmytro Bavol,[a] Werner M. Nau,[b] Detlef Gabel[b] and Bohumír Grűner*[a]

[a]Institute of Inorganic Chemistry, Czech Academy of Sciences, 25068 Řež, Czech Republic
[b]Jacobs University Bremen, 28759 Bremen, Germany
[c]Al-Balqa Applied University, Al-Salt 19117, Jordan
[d] University of Pardubice, Studentská 95, Pardubice, Czech Republic.

Table of Contents

1. **Materials and Methods** 2
2. **Experimental Part** 4
3. **Crystallographic results** 12
4. **ITC experiments** 15
5. **NMR Spectra** 18
6. **ESI Mass Spectra** 44

1. Materials and Methods

Experimental

General: Acetonitrile and dichloromethane were dried over molecular sieves (4 Å, Fluka), anhydrous K_2CO_3 (Lachner) was used. Other chemicals and solvents were from Aldrich, Merck, Lachner a.s. and Penta Ltd., Czech Republic, respectively, and were used without purification.

Instrumental Techniques

- **NMR spectra** were measured on Jeol 600 MHz spectrometer. The spectra of all compounds were measured immediately after dissolution in particular deuterated solvent, usually acetonitrile-d_3 unless otherwise stated. ^{11}B NMR (192 MHz) chemical shifts are given in ppm to high-frequency (low field) to $F_3B{\cdot}OEt_2$ as the external reference. Residual solvent ^{1}H resonances were used as internal secondary standards. The NMR data are presented in the text as follows: ^{11}B NMR: ^{11}B chemical shifts δ (ppm), multiplicity. ^{1}H NMR (600 MHz) and ^{13}C (150 MHz): chemical shifts δ are given in ppm relative to Me_4Si (0 ppm) as the external standard, coupling constants $J(H,H)$ are in Hz.

- **Mass spectrometry measurements** were performed on a Thermo-Finnigan LCQ-Fleet Ion Trap instrument using electrospray ionization (ESI) for ionic species or atmospheric pressure chemical ionization (APCI) for neutral carborane derivatives with detection of negative or positive ions, respectively. Samples dissolved in acetonitrile (concentrations approximately 100 ng.ml^{-1}) were introduced in case of ESI to the ion source by infusion of 6 µL/ min, source voltage 3.2 kV, tube lens voltage -90.7 V, capillary voltage -32.0 V, capillary temperature was 360°C, drying gas flow 7 L/ min. In most cases the negative ions corresponding to the molecular ion were observed with 100% abundance for the highest peak in the isotopic distribution plot. Molecular ions $[M]^-$ were detected for all univalent anions as the base peaks in the spectra. The isotopic distribution

in the boron plot of all peaks is in perfect agreement with the calculated spectral pattern. The data are presented for the most abundant mass in the boron isotopic distribution plot (100%).

Elemental Analysis. The samples of Me_4N^+ salts for Elemental Analysis (EA) were dried in vaccum at 98 ^oC for 7 h. EA was performed in the following analyzer: Thermo Scientific FlashSmart^{TM} 2000 Elemental analyzer (United States). The combustion tube packing was supplied with the instrument and consisted of the following components: EA-2000 chromium oxidizer, high quality copper reducer, and silver cobaltous-cobaltic oxide. Analysis of the sample; portions of samples with a mass around 1 mg were weighed in tin containers together with a vanadium pentoxide (10 mg). All the determinations were done in triples.

X-ray crystallography. The X-ray data for the compound **3** (colourless crystals by slow evaporation of a methanol/water solution) was collected at 150(2)K with a Bruker D8-Venture diffractometer equipped with Mo (Mo/K_α radiation; λ = 0.71073 Å) microfocus X-ray (IμS) source, Photon CMOS detector and Oxford Cryosystems cooling device was used for data collection. The frames were integrated with the Bruker SAINT software package using a narrow-frame algorithm. Data was corrected for absorption effects using the Multi-Scan method (SADABS). Obtained data were treated by XT-version 2014/5 and SHELXL-2017/1 software[1, 2] implemented in APEX3 v2016.9-0 (Bruker AXS) system. In compound **3**$^-$ there is a disorder of countercation K^+ (50:50), some fragments of complexes and solvent molecules (H_2O). H atoms of $[-N(H_2)-]^+$ fragments and H_2O were found from the Fourier difference electron density map, other H atoms were placed at calculated positions and refined in the ‘‘riding model”. $R_{int} = \sum|F_o^2 - F_{o,mean}^2|/\sum F_o^2$, $S = [\sum(w(F_o^2 - F_c^2)^2)/(N_{diffrs} - N_{params})]^{½}$ for all data, $R(F) = \sum||F_o| - |F_c||/\sum|F_o|$ for observed data, $wR(F^2) = [\sum(w(F_o^2 - F_c^2)^2)/(\sum w(F_o^2)^2)]^{½}$ for all data. Crystallographic data for structural analysis have been deposited with the Cambridge Crystallographic Data Centre, CCDC no. 1881515. Copies of this information may be obtained free of charge from The Director, CCDC, 12 Union Road, Cambridge CB2 1EY, UK (fax: +44-1223-336033; e-mail: deposit@ccdc.cam.ac.uk or www: http://www.ccdc.cam.ac.uk).

2. Experimental Part

- **<u>Isolation of crude epoxides Me_4N [$CH_2OCHCH_2NH_2B_{10}X_9$] (I-III)</u>**

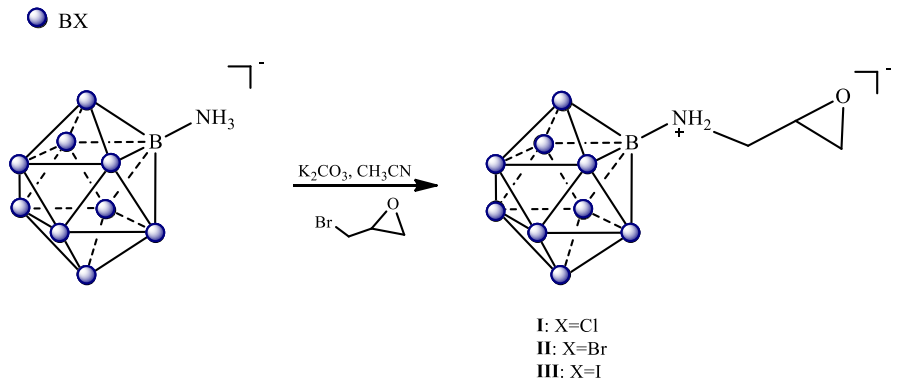

Me_4N[2-$NH_3B_{10}X_9$] (0.3 g, 1 equivalent) was dissolved in dry acetonitrile and K_2CO_3 (3 equivalents for X = Cl, Br and 6 equivalents for X=I) was added and the slurry was stirred at room temperature for 1 h. 1-bromo-2,3-epoxypropane (1.5 equivalent for X= Cl, Br and 4 equivalents for X=I) was then added by syringe and the reaction mixture was heated to 60-70 ^oC and followed by MS. When MS analysis of the crude sample showed majority of Me_4N [$CH_2OCHCH_2NH_2B_{10}X_9$]$^-$ (X= Cl, Br, I), the reaction was stopped and after cooling down the solution was passed *via* syringe through SPE Si cartridge (3x 1cm, Supelco) and evaporated to dryness. This procedure enabled to obtain crude products **I-III** of formulation [(2,3-μ-O-$CH_2CHCH_2)_2NHB_{10}X_9$] (X= Cl, Br, I) that still contained traces of unreacted starting compound and some minor side products. Crystallization was inefficient to remove impurities. Attempts at separation of the main products from impurities using chromatography on a short silica gel or neutral alumina led to almost complete decomposition of the products. On alumina, presence of dimer of molecular mass [$CH_2OCHCH_2NH_2B_{10}X_9$]$_2$ was observed by MS as almost sole product, which apparently formed in contact with column material. The instability of the oxirane ring towards chromatographic supports thus precluded isolation of pure compounds. Below we list ^{11}B, ^1H and ^{13}C NMR signals corresponding to crude products **I-III**. ^1H NMR spectra correspond

to set of the diastereotopic protons for CH_2 and two CH groups typical for the presence of an epoxide ring.

I. **$Me_4N[CH_2OCHCH_2NH_2B_{10}Cl_9]$ (I^-):** yellow solid, δB (192 MHz; CD_3CN; $F_3B.OEt_2$) -3.6 (s), -6.4 (s), {-10.5, -11.5, -12.1, -12.7} (s), -15.8 (s) ppm. δH(600 MHz; CD_3CN; Me_4Si) 3.42 (1H, dd, J= 13.4 Hz), 3.17-3.20 (1H, m), 3.05 (s, Me_4N^+), 2.803 (t, J= 5 Hz), 2.6 (1H, dd, J= 4, 2 Hz). δC(150 MHz; CD_3CN; Me_4Si) 55.5, 55.3, 48.8, 48.1, 46.2 ppm. MS (ESI$^-$): 500.08 (100 %); calcd. for $[CH_2OCHCH_2NH_2B_{10}Cl_9]$: 500.28 (100 %).

II. **$Me_4N[CH_2OCHCH_2NH_2B_{10}Br_9]$ (II^-):** white solid; δB (192 MHz; CD_3CN; $F_3B.OEt_2$) {-3.5, -4.6} (s), -7.2 (s), {-11.3, -13.0, -14.3, -16.8} (s) ppm. δH(600 MHz; CD_3CN; Me_4Si) 3.53 (1H, dd, J= 11, 4 Hz), 3.29 (1H, dd, J= 11, 6 Hz), 3.18-3.21 (1H, m), 3.06 (s, Me_4N^+), 2.85 (1H, t, J= 5 Hz), 2.62 (1H, dd, J= 2, 5 Hz). δC(150 MHz; CD_3CN; Me_4Si) 55.5, 53.5, 50.01, 48.1 ppm. MS (ESI$^-$): 900.76 (100 %); calcd. for $[CH_2OCHCH_2NH_2B_{10}Br_9]^-$: 900.34 (100 %).

III. **$Me_4N[CH_2OCHCH_2NH_2B_{10}I_9]$ (III^-):** yellow solid, δB (192 MHz; CD_3CN; $F_3B.OEt_2$) -3.6 (s), -5.8 (s), {-9.9, -10.8, -12.9} (s), {-17.8, -19.2, -20.1, -20.9, -22.4, -2.99} (s) ppm. δH(600 MHz; CD_3CN; Me_4Si) 3.53 (1H, dd, J= 11, 5 Hz), 3.29 (1H, dd, J= 11, 8 Hz), 3.18-3.21 (1H, m), 3.07 (s, Me_4N^+), 2.85 (1H, t, J= 5 Hz), 2.62 (1H, dd, J= 2, 5 Hz). δC(150 MHz; CD_3CN; Me_4Si) 55.6, 50.8, 47.2, 45.3 ppm. MS (ESI$^-$): 661.4 (100%); calcd. for $[CH_2OCHCH_2NH_2B_{10}I_9]^{2-}$: 661.65 (100%).

- **<u>One pot reaction of $Me_4N[B_{10}X_9NH_2CH_2CHOCH_2]$ with amines:</u>**

The acetonitrile solution of crude epoxide **I-III** prepared according the previous paragraph was used. The amine in excess (1 mL) was added directly to this solution and kept heating at 60 ^oC for17 h. The undissolved K_2CO_3 were removed by filtration and the filtrate was concentrated under reduced pressure to provide the crude product, which was purified by column chromatography using CH_2Cl_2/CH_3CN (from 5: 1 to 1: 1, b.v.) as eluent to afford the pure

product. This purification was done several times to remove all the impurities. The fractions containing the products after chromatography were dissolved in aqueous MeOH and precipitated by excess of Me_4NCl. The pure fraction was then recrystallized from water/methanol and characterized by NMR (^{11}B, ^{1}H and ^{13}C), LC-MS and elemental analysis and other techniques.

– **<u>Reaction of $Me_4N[B_{10}X_9NH_2CH_2CHOCH_2]$ with primary amine (Butyl amine):</u>**

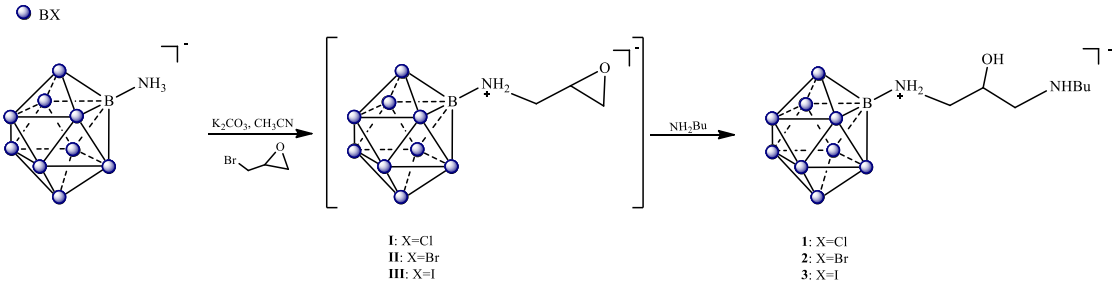

1. **$Me_4N[B_{10}Cl_9NH_2CH_2CH(OH)CH_2NH(CH_2)_3CH_3]$ (1^-):** Yield 0.149 g (40 %), white solid; δB(192 MHz; CD_3CN; $F_3B.OEt_2$) -3.5 (1 B, s), -6.2 (1 B, s), -10.6, -11.5, -12.2 (7 B, s), -15.98 (1 B, s) ppm. δH(600 MHz; CD_3CN; Me_4Si) 8.75 (1 H, br s, N*H*), 8.46 (1 H, br s, N*H*), 6.71 (1 H, br s, N*H*), 6.03 (1 H, s, O*H*), 5.69 (1 H, br s, N*H*), 4.401 (1 H, br., $NH_2CH_2CH(OH)CH_2$), 3.39 (1 H, br., $NH_2CH_2CH(OH)CH_2$), 2.85-3.17 (17 H, s+m, $(CH_3)_4N^+$ + $NH_2CH_2CH(OH)CH_2NHCH_2CH_2CH_2CH_3$), 1.65-1.703 (2 H, m, $NHCH_2CH_2CH_2CH_3$), 1.33-1.39 (2 H, m, $NHCH_2CH_2CH_2CH_3$), 0.903 (3 H, t, J=7.5 Hz, $NHCH_2CH_2CH_2CH_3$) ppm. δC(150 MHz; CD_3CN; Me_4Si) 63.7 ($NH_2CH_2CH(OH)CH_2$), 55.3 (4C, Me_4N^+), 51.4 $NH_2CH_2CH(OH)CH_2$, 48.3 ($NHCH_2CH_2CH_2CH_3$), 48.01 $NH_2CH_2CH(OH)CH_2$, 27.5 ($NHCH_2CH_2CH_2CH_3$), 19.5 ($NHCH_2CH_2CH_2CH_3$), 12.9 ($NHCH_2CH_2CH_2CH_3$) ppm; MS (ESI^-): 572.42 (100%); calcd. for $[B_{10}Cl_9NH_2CH_2CH(OH)CH_2NH(CH_2)_3CH_3]^-$: 573.42 (100%). Anal. found: C, 20.0; H, 4.7; N, 6.3. Calc. for $Me_4N[B_{10}Cl_9NH_2CH_2CH(OH)CH_2NH(CH_2)_3CH_3]$: C, 20.4; H, 4.7; N, 6.5%.

2. **$Me_4N[B_{10}Br_9NH_2CH_2CH(OH)CH_2NH(CH_2)_3CH_3]$ (2^-):** Yield 0.176 g, (52 %), white solid; δB (192 MHz; CD_3CN; $F_3B.OEt_2$) -2.7 (1 B, s), -6.6 (1 B, s), -13.7, -14.3, -14.9 (8 B, s) ppm; δH (600 MHz; CD_3CN; Me_4Si) 7.49 (1 H, s, N*H*), 7.17 (1 H, s, N*H*), 5.97 (1

H, s, N*H*), 5.41 (1 H, s, N*H*), 5.04 (1 H, s, O*H*), 4.22 (1H, br., $NH_2CH_2C\mathit{H}(OH)CH_2$), 3.53 (1H, br., $NH_2C\mathit{H}_2CH(OH)CH_2$), 2.89-3.12 (17 H, s+m, $(C\mathit{H}_3)_4N^+$ + $NH_2C\mathit{H}_2CH(OH)C\mathit{H}_2NHC\mathit{H}_2CH_2CH_2CH_3$), 1.60-1.65 (m, 2H, $NHCH_2C\mathit{H}_2CH_2CH_3$), 1.32-1.38 (m, 2H, $NHCH_2CH_2C\mathit{H}_2CH_3$), 0.905 (t, 3H, J=7.6 Hz, $NHCH_2CH_2CH_2C\mathit{H}_3$) ppm; δC (150 MHz; CD_3CN; Me_4Si) 63.4 ($NH_2CH_2\mathit{C}H(OH)CH_2$), 55.2 (4C, Me_4N^+), 50.6 ($NH_2CH_2CH(OH)\mathit{C}H_2$), 48.2 ($NH\mathit{C}H_2CH_2CH_2CH_3$), 47.7 ($NH_2\mathit{C}H_2CH(OH)CH_2$) , 27.4 ($NHCH_2\mathit{C}H_2CH_2CH_3$), 19.4 ($NHCH_2CH_2\mathit{C}H_2CH_3$), 12.8 ($NHCH_2CH_2CH_2\mathit{C}H_3$) ppm; MS (ESI$^-$): 974.0 (100%); calcd. for $[B_{10}Br_9NH_2CH_2CH(OH)CH_2NH(CH_2)_3CH_3]^-$: 973.48 (100 %); Anal. Found: C, 12.6; H, 2.9; N, 4.1. Calc. for $Me_4N[B_{10}Br_9NH_2CH_2CH(OH)CH_2NH(CH_2)_3CH_3]$ C, 12.6; H, 2.9; N, 4.0%.

3. **$Me_4N[B_{10}I_9NH_2CH_2CH(OH)CH_2NH(CH_2)_3CH_3]$ (3^-):** Yield 0.188 g (57%), light yellow crystals; δB (192 MHz; CD_3CN; $F_3B.OEt_2$) -3.6 (1 B, s), -10.3 (1 B, s), -14.2 (1 B, s), -20.2, -21.7, -23.5 (7 B, s) ppm. δH (600 MHz; CD_3CN; Me_4Si) 8.10 (1 H, br s, N*H*), 7.59 (1 H, br s, N*H*), 6.00 (1 H, br s, N*H*), 5.58 (1 H, s, O*H*), 5.19 (1H, br s, N*H*), 4.33 (1 H, br., $NH_2CH_2C\mathit{H}(OH)CH_2$), 3.7 (1 H, br., $NH_2C\mathit{H}_2CH(OH)CH_2$), 2.85-3.18 (17 H, s+m, $(C\mathit{H}_3)_4N^+$ + $NH_2C\mathit{H}_2CH(OH)C\mathit{H}_2NHC\mathit{H}_2CH_2CH_2CH_3$), 1.63-1.68 (2 H, m, $NHCH_2C\mathit{H}_2CH_2CH_3$), 1.33-1.39 (2 H, m, $NHCH_2CH_2C\mathit{H}_2CH_3$), 0.904 (3 H, t, *J*= 7.2 Hz, $NHCH_2CH_2CH_2C\mathit{H}_3$). δC (150 MHz; CD_3CN; Me_4Si) 63.1 ($NH_2CH_2\mathit{C}H(OH)CH_2$), 55.3 (4C, Me_4N^+), 51.1 ($NH_2CH_2CH(OH)\mathit{C}H_2$), 48.2 ($NH\mathit{C}H_2CH_2CH_2CH_3$), 46.7 $NH_2\mathit{C}H_2CH(OH)CH_2$, 27.5 ($NHCH_2\mathit{C}H_2CH_2CH_3$), 19.4 ($NHCH_2CH_2\mathit{C}H_2CH_3$), 12.9 ($NHCH_2CH_2CH_2\mathit{C}H_3$) ppm; MS (ESI$^-$): 1396.50; calcd. for $[B_{10}I_9NH_2CH_2CH$-$(OH)CH_2NH(CH_2)_3CH_3]^-$: 1396.48; Anal. found: C, 8.9; H, 2.1; N, 2.8. Calc. for $Me_4N[B_{10}I_9NH_2CH_2CH(OH)CH_2NH(CH_2)_3CH_3]$: C, 9.0; H, 2.1; N, 2.9%.

– **<u>Reaction of $Me_4N[B_{10}X_9NH_2CH_2CHOCH_2]$ with secondary amine (Diethyl amine):</u>**

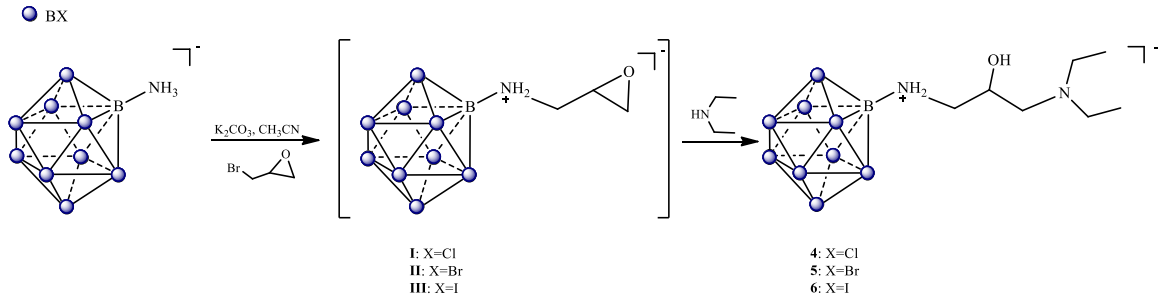

4. **$Me_4N[B_{10}Cl_9NH_2CH_2CH(OH)CH_2N(CH_2CH_3)_2]$ (4^-):** Yield 0.179 g (79%), yellowish solid, δB (192 MHz; CD_3CN; $F_3B.OEt_2$) -3.4 (1 B, s), -6.3 (1 B, s), -10.4, -11.5, -12.2 (7 B, s), -16.03 (1 B, s) ppm; δH (600 MHz; CD_3CN; Me_4Si) 8.97 (1 H, br s, N*H*), 5.95 (1 H, br s, N*H*), 5.62 (1 H, br s, N*H*), 5.51 (1 H, s, N*H*), 4.30 (1 H, br., $NH_2CH_2CH(OH)CH_2$), 3.43 (1H, $NH_2CH_2CH(OH)CH_2$), 2.99-3.24 (19 H, s+m, $(CH_3)_4N^+$ + $NH_2CH_2CH(OH)$- $CH_2N(CH_2CH_3)_2$), 1.27 (t, 3H, *J*= 7.5 Hz, $N(CH_2CH_3)_2$), 1.26 (t, 3H, *J*= 8.0 Hz, $N(CH_2CH_3)_2$); δC (150 MHz; CD_3CN; Me_4Si) 62.63 (NH_2CH_2**C**$H(OH)CH_2$), 56.02, 55.32 (4C, Me_4N^+), 49.45, 48.14, 47.74, {8.23, 7.88} (2C, $N(CH_2CH_3)_2$). MS (ESI^-): 574.12; calcd. for $[B_{10}Cl_9NH_2CH_2$-$CH(OH)CH_2N(CH_2CH_3)_2]^-$ 573.41; Anal. found: C, 20.6; H, 4.8; N, 6.6; Calc. for $Me_4N[B_{10}Cl_9NH_2CH_2CH(OH)CH_2N(CH_2CH_3)_2]$ C, 20.4; H, 4.7; N, 6.5%.

5. **$Me_4N[B_{10}Br_9NH_2CH_2CH(OH)CH_2N(CH_2CH_3)_2]$ (5^-):** Yield 0.210 g, (61%), light yellowish solid; δB (192 MHz; CD_3CN; $F_3B.OEt_2$) -2.7 (1 B, s), -6.5 (1 B, s), -13.6, -14.4, -15.1 (8 B, s) ppm; δH (600 MHz; CD_3CN; Me_4Si) 9.91 (1 H, br s, N*H*), 6.08 (1 H, s, O*H*), 5.91 (1 H, br s, N*H*), 5.42 (1 H, br s, N*H*), 4.34 (1H, br., $NH_2CH_2CH(OH)CH_2$), 3.57 (1H, br., $NH_2CH_2CH(OH)CH_2$), 2.97-3.23 (s+m, 19H, $(CH_3)_4N^+$ + $NH_2CH_2CH(OH)CH_2$- $N(CH_2CH_3)_2$), 1.289 (t, 3H, *J*= 7.5 Hz, $N(CH_2CH_3)_2$), 1.27 (t, 3H, *J*= 7.5 Hz, $N(CH_2CH_3)_2$). δC(150 MHz; CD_3CN; Me_4Si) 62.56 ($NH_2CH_2CH(OH)CH_2$), 55.30 (4C, Me_4N^+), 57.49, 49.30, 47.99 ($NH_2CH_2CH(OH)CH_2N(CH_2CH_3)_2$), 47.07 ($NH_2CH_2CH(OH)CH_2$), {8.13, 8.03} (2C, $N(CH_2CH_3)_2$). MS (ESI^-): m/z = 1396.50;

calcd. for $[B_{10}I_9NH_2CH_2CH(OH)CH_2N(CH_2CH_3)_2]^-$: 1396.48; Anal. found: C, 12.6; H, 3.1; N, 4.2. Calc. for $Me_4N[B_{10}Br_9NH_2CH_2CH(OH)CH_2N(CH_2CH_3)_2]$: C, 12.6; H, 3.0; N, 4.0%.

6. **$Me_4N[B_{10}I_9NH_2CH_2CH(OH)CH_2N(CH_2CH_3)_2]$ (6^-):** Yield 0.19 g (58%), dark yellowish solid; δB (192 MHz; CD_3CN; $F_3B.OEt_2$) -3.6 (1 B, s), -10.3 (1 B, s), -14.1 (1 B, s), -20.2, -21.6, -23.6 (7 B, s) ppm. δH (600 MHz; CD_3CN; Me_4Si) 9.05 (1 H, br s, N*H*), 5.84 (1 H, br s, N*H*), 5.66 (1 H, s, O*H*), 5.25 (1 H, br s, N*H*), 4.36 (1 H, br., $NH_2CH_2C\mathit{H}(OH)CH_2$), 3.73 (1 H, br., $NH_2C\mathit{H}_2CH(OH)CH_2$), 3.001-3.21 (19 H, s+m, $(C\mathit{H}_3)_4N^+$ + $NH_2C\mathit{H}_2CH(OH)C\mathit{H}_2N(C\mathit{H}_2CH_3)_2$), 1.27 (t, 3H, J= 6.9 Hz, $N(CH_2C\mathit{H}_3)_2$), 1.26 (t, 3H, J= 6.9 Hz, $N(CH_2C\mathit{H}_3)_2$). δC(150 MHz; CD_3CN; Me_4Si) 62.12 ($NH_2CH_2\mathit{C}H(OH)CH_2$), {56.38, 49.50, 47.82} ($NH_2CH_2CH(OH)\mathit{C}H_2N(C\mathit{H}_2CH_3)_2$), 55.36 (4C, Me_4N^+), 46.47 ($NH_2\mathit{C}H_2CH(OH)CH_2$), {8.32, 8.03} (2C, $N(CH_2\mathit{C}H_3)_2$). MS (ESI$^-$): 1396.50; calcd. for $[B_{10}I_9NH_2CH_2CH(OH)CH_2N(CH_2CH_3)_2]^-$: 1396.48; Anal. found: C, 8.7; H, 2.0; N, 2.8; Calc. for $Me_4N[B_{10}I_9NH_2CH_2CH(OH)CH_2N(CH_2CH_3)_2]$: C, 9.0; H, 2.2; N, 2.9%.

<u>Reaction of $Me_4N[B_{10}Br_9NH_2CH_2CHOCH_2]$ with benzyl amine</u>

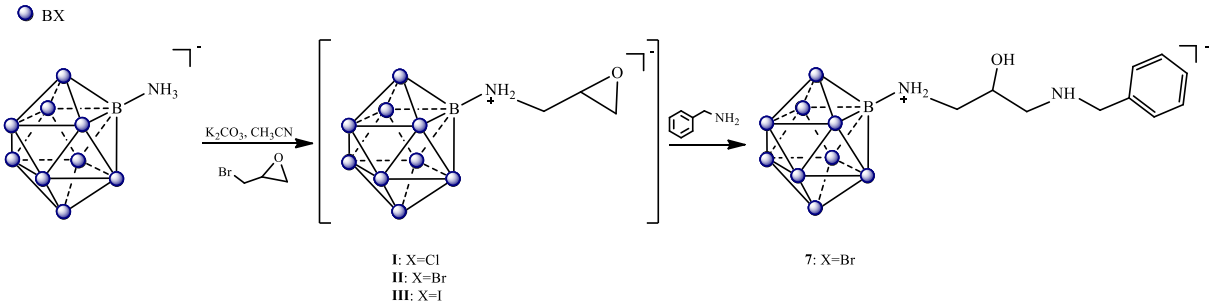

7. **$Me_4N[B_{10}Br_9NH_2CH_2CH(OH)CH_2NHCH_2Ph]$ (7^-):** Yield 0.115 g (43%), white solid; δB(192 MHz; CD_3CN; $F_3B.OEt_2$) -2.6 (1 B, s), -6.6 (1 B, s), -13.6, -14.3, -14.9 (8 B, s) ppm. δH(600 MHz; CD_3CN; Me_4Si) 8.007 (1 H, br s, N*H*), 7.797 (1 H, br s, N*H*), 7.42-

7.498 (m, 5H, C_6H_5), 6.03 (1 H, br s, N*H*), 5.42 (1 H, br s, N*H*), 5.05 (1 H, s, OH), 4.258 (1H, $NH_2CH_2CH(OH)CH_2$), 4.16 (s, $NHCH_2Ph$), 3.49 (1H, $NH_2CH_2CH(OH)CH_2$), 2.911-3.107 (s+m, 15 H, $(CH_3)_4N^+$ + $NH_2CH_2CH(OH)CH_2N(CH_2CH_3)_2$). ^{13}C NMR (Acetonitrile-d_3): δC = {130.43, 130.35, 129.797, 129.15} (C_6H_5), 63.48 ($NH_2CH_2CH(OH)CH_2$), 55.32 (4C, Me_4N^+), 51.56, 50.14, 47.74 (CH_2); MS (ESI$^-$): 1008.68; calcd. for $[B_{10}Br_9NH_2CH_2CH(OH)CH_2NHCH_2Ph]^-$: 1007.49; Anal found: C, 15.5; H, 2.8; N, 3.7. Calc. for $Me_4N[B_{10}Br_9NH_2CH_2CH(OH)CH_2NHCH_2Ph]$: C, 15.6; H, 2.6; N, 3.9%.

<u>Reaction of $Me_4N[B_{10}Br_9NH_2CH_2CHOCH_2]$ with O-nucleophile (2-methoxyphenol)</u>

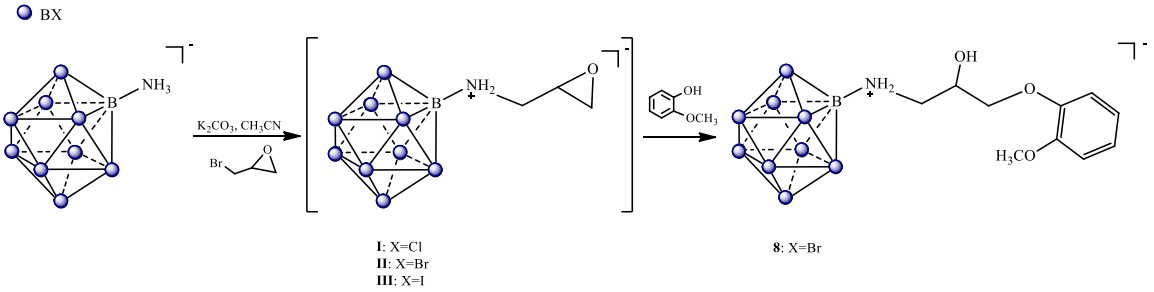

8. $Me_4N[2\text{-}NH_3B_{10}Br_9]$ (0.224 g, 0.244 mmol) was dissolved in dry acetonitrile and K_2CO_3 (0.115 g, 0.832 mmol) was added and the slurry was stirred at room temperature for 1 h. 1-bromo-2,3-epoxypropane (30 µL, 0.35 mmol) was then added by syringe and the reaction mixture was heated to 60 ^oC and followed by MS. When MS analysis of the crude sample showed majority of Me_4N $[CH_2OCHCH_2NH_2B_{10}Br_9]$, 1 mL of 2-methoxyphenol ($9.09*10^{-3}$ mol) deprotonated with NaH (0.371 g, 0.0155 mol) in distilled THF was added to the reaction mixture followed by addition of 0.1 g of K_2CO_3. The mixture was heated to 60 ^oC for 4 days. The undissolved K_2CO_3 were removed by filtration and the filtrate was concentrated under reduced pressure to provide the crude product, which was purified by column chromatography using CH_2Cl_2/CH_3CN as eluent. This purification was done twice to remove most of the impurities. The pure fraction was recrystallized from water/methanol. The solid obtained was also recrystallized by DCM/hexane to remove the remaining impurities.

$Me_4N[B_{10}Br_9NH_2CH_2CH(OH)CH_2OC_6H_4OCH_3]$ (8^-): Yield 0.137 g (51%), yellowish solid; δB(192 MHz; CD_3CN; $F_3B.OEt_2$) -2.4 (s, 1B), -6.7 (s, 1B), -13.5, -14.5, -14.99 (s, 8B) ppm; δH(600 MHz; CD_3CN; Me_4Si) 6.85-7.004 (4 H, m, C_6H_4), 5.79 (1H, br s, N*H*), 5.65 (1 H, s, O*H*), 5.56 (1 H, br s, N*H*), 4.125-4.154 (1 H, NH_2CH_2C*H*$(OH)CH_2$), 3.97-4.002, 4.08-4.107 (2H, dd, $NH_2CH_2CH(OH)C$*H*$_2$), 3.77 (3H, s, OCH_3), 3.44-3.65 (2H, 2m, NH_2C*H*$_2CH(OH)CH_2$), 3.04 (12 H, s, $(CH_3)_4N^+$; δC(150 MHz; CD_3CN; Me_4Si) 122.4, 120.8, 120.8, 114.5, 112.4, 112.2 (ph), 72.2, 65.3, 55.6, 55.3, 48.8. MS (ESI$^-$): m/z = 1024.68; calcd. for $Me_4N[B_{10}Br_9NH_2CH_2CH(OH)CH_2OC_6H_4OCH_3]$:.1024.46; Anal found: C, 15.4; H, 2.5; N, 2.6. Calc. for $Me_4N[B_{10}Br_9NH_2CH_2CH(OH)CH_2OC_6H_4OCH_3]$: C,15.3; H, 2.6; N, 2.55%.

Acid-base properties of the corresponding amines and influence on Chemical Shifts in NMR .

The amines **1^- to 7^-** have, in principle, two amine functions that can be protonated of deprotonated. Particularly, the protonation/ deprotonation group sitting directly at B(2) of the cage may show high shielding/ deshielding effect on NMR shifts of this and other boron atoms in the cage. The NH_2- groups attached directly to boron atoms of the cage anions are basic tend to be protonated during aqueous workup and isolation. If not stated otherwise, all chemical shifts in ^{11}B, ^{1}H and ^{13}C NMR spectra given in this Experimental part thus correspond to form, where the basic B(2)-NR_2 function is protonated. As has been reported recently for parent series of halogenated 2-ammonio decaborate ions that were unsubstituted at ammonio group,[3] the deprotonation causes appreciable shifts of the ^{11}B NMR signals of all atoms in the spectrum, the most shifted being the peaks for B(2) and B(10) and the position B(4). The similar effect can be observed also within the current series and could be enhanced by protonation of the second RNH or R_2N function in the aliphatic chain at low pH values. Examples for ^{11}B NMR spectra of deprotonated/ protonated couples of compounds $Me_4N[B_{10}X_9NH_2CH_2CH(OH)CH_2NH(CH_2)_3CH_3]$ are shown in Figs. S25 and S26 for X= Cl or I.

3. Crystallographic results

Crystallographic data for hydrated double salt of formulation Me_4NK(**3).5.5 H_2O**: ($B_{10}I_9ON_2C_7H_{18}$, K, $B_{10}I_9ON_2C_7H_{18}$, $N(CH_3)_4$ and $5.5 \cdot H_2O$), M = 3005.20, triclinic, P-1, a = 10.1189(10), b = 20.238(2), c = 22.110(3) Å, α = 64.047(3), β = 88.647(3), γ = 82.635(3)°, Z = 2, V = 4035.0(8) Å^3, D_c = 2.474 g.cm^{-3}, μ = 6.984 mm^{-1}, T_{min}/T_{max} = 0.0540/0.1656; $-13 \leq h \leq 13$, $-26 \leq k \leq 26$, $-29 \leq l \leq 29$; 173594 reflections measured (θ_{max} = 27.999°), 19483 independent (R_{int} = 0.0783), 15564 with $I > 2\sigma(I)$, 722 parameters, S = 1.028, R_1(obs. data) = 0.0607, wR_2(all data) = 0.1041; max., min. residual electron density = 1.892, -1.763 eÅ^{-3}.

Table 1 Selected interatomic distances and angles in the structure of **Me_4NK(3).5.5 H_2O**

Atom	Atom	Distance [Å]
B1	**B2**	**1.71(1)**
B1	**B4**	**1.69(1)**
B2	**B3**	**1.85(1)**
B2	**B5**	**1.838(9)**
B2	**B9**	**1.80(1)**
B3	**B7**	**1.81(1)**
B5	**B9**	**1.83(1)**
B9	**B10**	**1.69(1)**
B2	**N1**	**1.53(1)**
B1	**I1**	**2.136(8)**
B3	**I3**	**2.182(8)**
B5	**I5**	**2.174(7)**
B6	**I6**	**2.182(7)**
C1	**N1**	**1.50(1)**
C1	**C2**	**1.54(1)**
C2	**O1**	**1.42(1)**
C2	**C3**	**1.50(1)**
C4	**N2**	**1.49(1)**
C4	**C5**	**1.57(3)**
H1	**N1**	**0.91(8)**

Interatomic angles	[°]
B1-B3-B2	57.6(4)
B1-B2-B6	111.3(6)
B8-B5-B9	60.1(4)
I1-B1-B2	130.0(5)
I1-B1-B6	130.5(5)
I6-B6-B7	134.6(5)
N1-B2-B1	120.4(6)
C1-N1-C2	116.1(6)
C3-C2-C1	107.2(7)
O1-C1-C2	108.7(8)
O1-C2-C3	111.9(8)
I6-K2-K1	62.4(1)
O1-K2-K1	132.8(4)

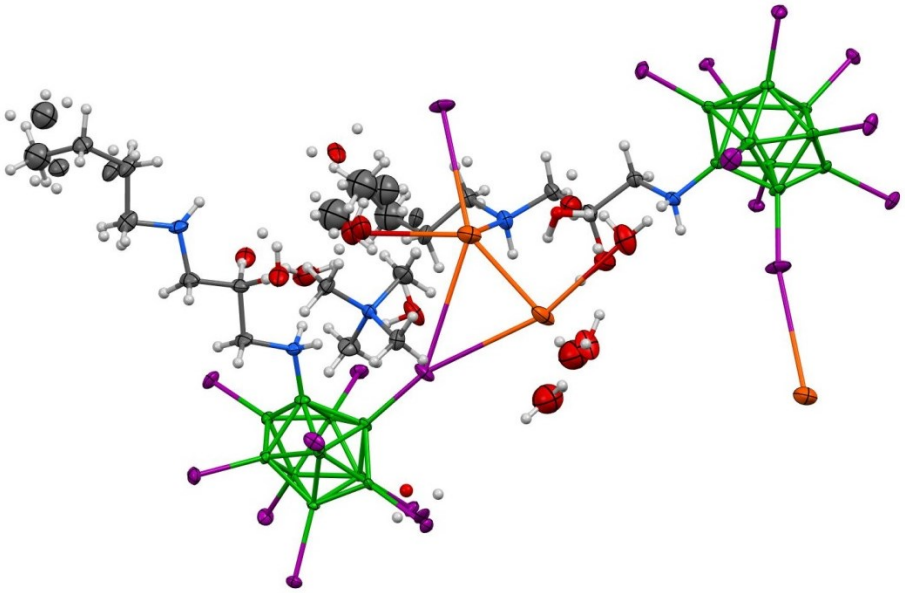

Fig. S1 The molecular structure of double salt K.**N**$(CH_3)_4$.$[B_{10}I_9ON_2C_7H_{18}]_2$ and 5.5·H_2O, **3**$^{-}$

The crystals of compound **3**$^-$ were colorless and were grown by cooling down a crude sample taken after initial workup of the reaction mixture before chromatography and precipitation of Me_4N^+ salt. This resulted in the presence of double salt containing along Me_4N^+ also the K^+ cation in equimolar ratio.

Unit cell contains two boron cages with the corresponding substitution with ammonio function, hydroxypropyl pendant group and terminal butyl amine. The substituent that originated from cleavage of the epoxide ring is inherently chiral. Both enantiomers are distributed equally and statistically occupy available positions in each unit cell of the racemic crystal.

Potassium cations are located two and two together in the channel in the structure in an endless chain along a axis with mean distance between two K^+ atoms is each couple 3.01 Å. Two hydrocarbon chains as well as two iodinated borate cages circumscribe the channel. The occupancy of the disordered potassium cations in both positions is one half, which makes the whole system neutral. Each of the potassium atoms has close contacts with terminal amino group that is substituted with butyl chain and is coordinated to water molecules. Noteworthy is the short contact with I(6) iodine atom sitting on B(6) of each cage with mean distance 3.80 Å. This atom is located in the equatorial position of the cage below the site of substitution by ammonium group.

The crystals for x-ray crystallography were grown from hot water, to which methanol was added for dissolution. This led to a presence of hydrate molecules in the structures. One water molecule was found in close proximity to each –OH, $–H_2N$ $–H_3N$ group. The molecular structure thus revealed an extensive supramolecular architecture *via* various H-bridges, particularly present in inner part of the substituent, either from the hydroxyl or ammonio group and water present within unit cells. There is no doubt the presence of a potassium cation and protic solvent is directly reflected in the structure controlling the construction of both hydrophilic and lipophilic parts of the cages to the particular sectors of the unit cell. Presence of water molecule was found to support also the structures of Me_4N^+ salts of parent compounds with unsubstituted ammonio group.[3]

Considering parent, nonhalogenated cages, the frequency of boron clusters compounds that contain nitrogen atom attached to boron atom is rather highly abundant in CCDC, the number of molecules bearing one or two hydrocarbon chains is limited to about fifty examples.

In fact, there is only one structure for borate ion from icosahedral series in which the ammonio function is substituted by only one alkyl substituent represented by 2-propane[4] found within the literature. In respect to polyhalogenated ions, approx. 25 structures correspond to halogenated amino/ ammonio derivatives, of which the vast majority belongs to the class of 12-vertex polyhalogenated *closo*-1-carbadodecaborates and *closo*-dodecaborates. Considering the latter compounds, 15 structures correspond to $[1\text{-}Me_3N\text{-}B_{12}X_{11}]^-$ (X= F, Cl)[5-8] and six to compounds with unsubstituted $[1\text{-}H_3N\text{-}B_{12}X_{11}]^-$ [7, 8] and $[1\text{-}H_3N\text{-}B_{10}X_9]^-$.[3]

With respect to the bonding situation the B-N separations and B-N-C interatomic angles in this and current structure are almost identical to those reported in[4] but the C-N bond lengths in 3^- is significantly longer due to the presence of the C-OH function. Similar distances and angles in the respect of the borate cage and ammonio function have been found in structures of 2-NH_3-substituted, nonahalogenated ten vertex borates published recently by us.[3]

4. ITC experiments

Experiments were carried out on a VP-ITC from MicroCal, Inc., at 25 °C. The binding equilibria were studied using 0.2 mM solution of cluster compound a cellular guest solution to which 5 mM γ-CD solution was titrated at 25 °C. Typically, 27 consecutive injections of 10 μL were used. All solutions were degassed prior to titration. Data were fitted with Origin 7.0 software according to a one-set-of-sites model. The knowledge of the complex stability constant (K_a) and molar reaction enthalpy ($\Delta H°$) enabled the calculation of the standard free energy ($\Delta G°$) and entropy changes ($\Delta S°$) according to $\Delta G° = -RT \ln K_a = \Delta H° - T\Delta S°$.

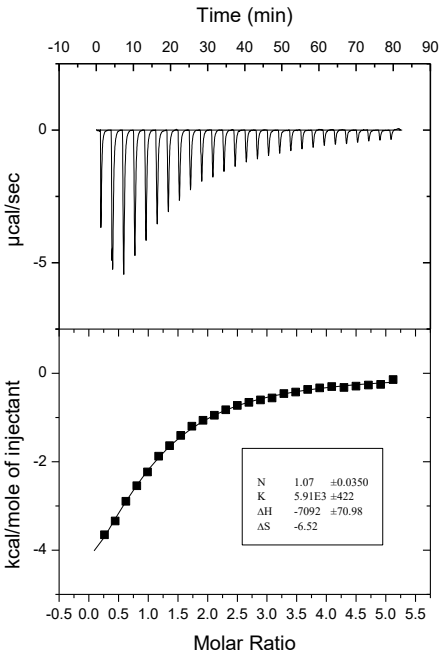

Fig. S2 $Me_4N[B_{10}Cl_9NH_3]$ and γ-CD

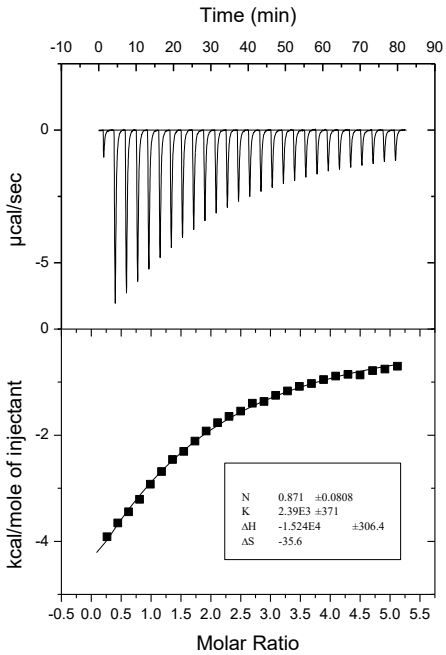

Fig. S3 $Me_4N[B_{10}Br_9NH_3]$ and γ-CD

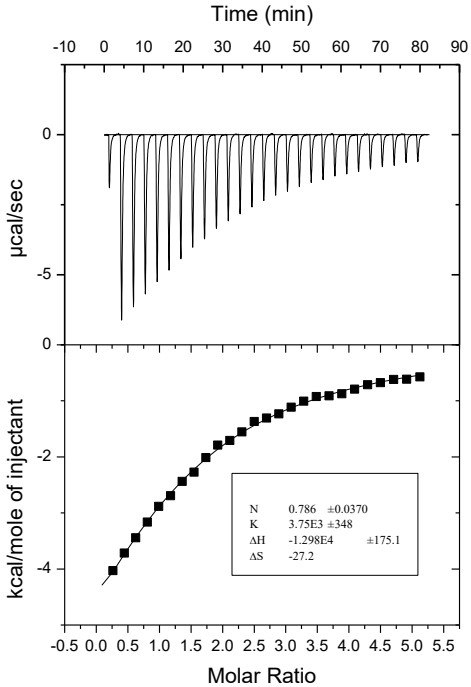

Fig. S4 $Me_4N[B_{10}I_9NH_3]$ and γ-CD

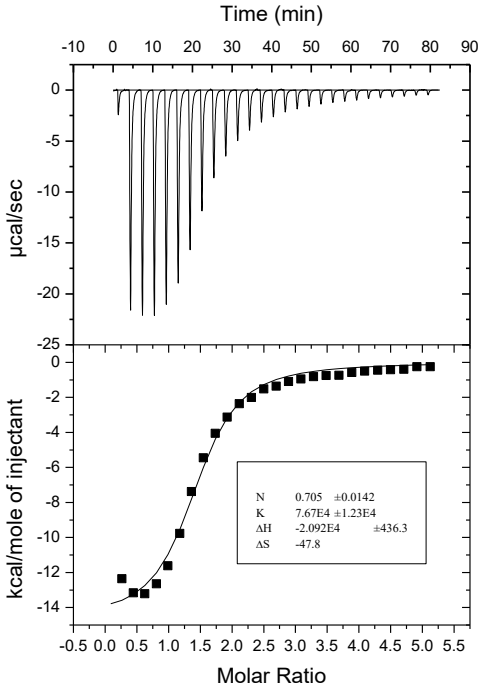

Fig. S5 $Me_4N[B_{10}Cl_9NMe_3]$ and γ-CD

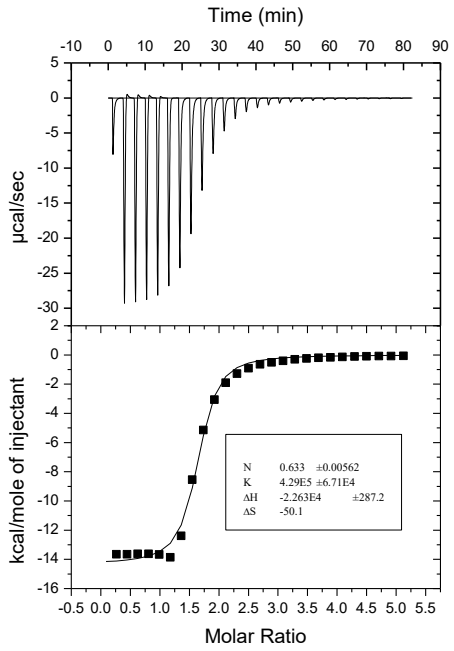

Fig. S6 $Me_4N[B_{10}Br_9NMe_3]$ and γ-CD

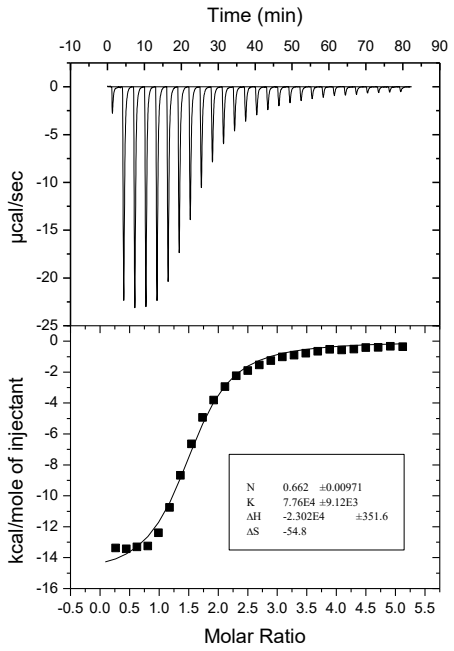

Fig. S7 $Me_4N[B_{10}I_9NMe_3]$ and γ-CD

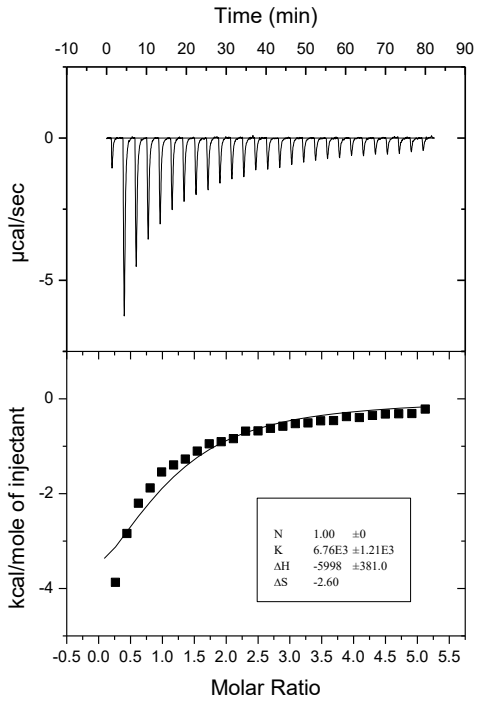

Fig. S8 Compound **1**$^-$ and γ-CD

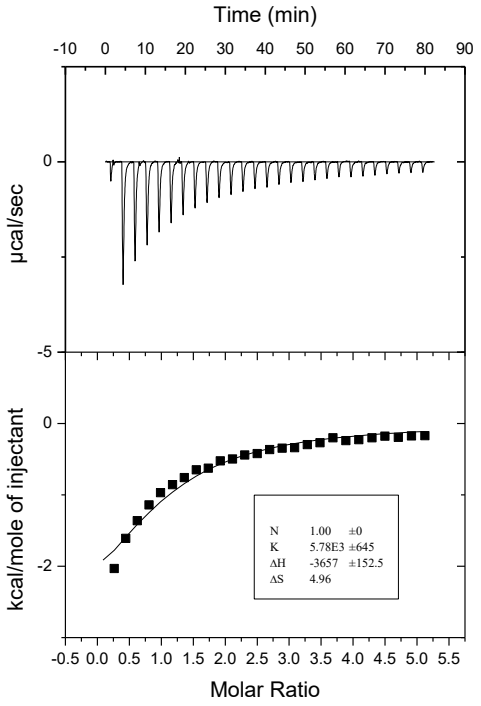

Fig. S9 Compound **2**$^-$ and γ-CD

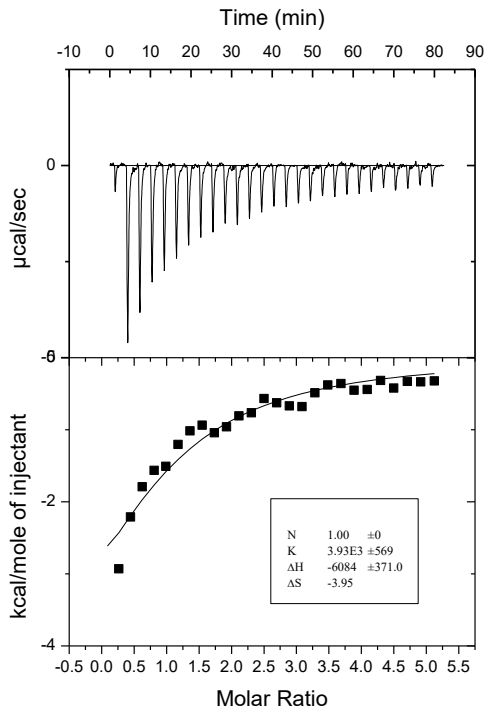

Fig. S10 Compound **3**$^-$ and γ-CD

5. NMR Spectra

- **Complexation of halogenated ammonio-decaborate derivatives with γ-CD**

The supramolecular host−guest complexation of substituted decaborates has not been yet systematically studied. The complexation of the tetramethyl ammonium salts of halogenated anions with γ-CD was investigated by means of ^{1}H NMR spectroscopy, which was possible due to their sufficient solubility in D_2O. ^{1}H NMR spectroscopy experiments were conducted for the guests from three series: a) $[H_3NB_{10}X_9]^-$, b) their methylated analogues $[Me_3NB_{10}X_9]^-$ and c) compounds, where the epoxide ring was opened with butyl amine $[B_{10}X_9NH_2CH_2CH(OH)CH_2NHBu]^-$ (X= Cl, Br, I), in D_2O (Figures S11, S12, and S13). Spectral changes following the addition of the synthesized borate derivatives were observed for all compounds under study. In particular, we observed a pronounced downfield complexation-induced shift of the H3 proton (Figures S11-S13), which is located inside the cavity near the

secondary (wider) hydroxyl rim, and serves as diagnostics signal for the formation of inclusion complexes. This shift increases for all three types of compounds from chloro- to bromo derivative and then, with exception of trimethylammonio- derivatives, decreases for iodo-substitution. Another diagnostic signal of H5 located near primary hydroxyl (narrower) rim is shifted significantly only in the case of chloro derivatives. Also the ^{1}H NMR signals of H2 and H4 and H1 show upfield shift with highest incremental value for corresponding bromo-derivatives and the series of anions substituted with Me_3N- group. The latter compounds show the largest complexation-induced chemical shifts (Δδ up to 0.25 ppm) almost comparable to halogenated dodecaborate ions and cobalt bis(dicarbollodes), which can be explained by a deeper immersion of the halogenated decaborate ions into the cavity of γ-CD. All complexes showed relatively slow exchange on the NMR spectroscopy timescale (ms), which resulted in peak broadening. This is the most apparent for the heaviest iodo-derivatives.

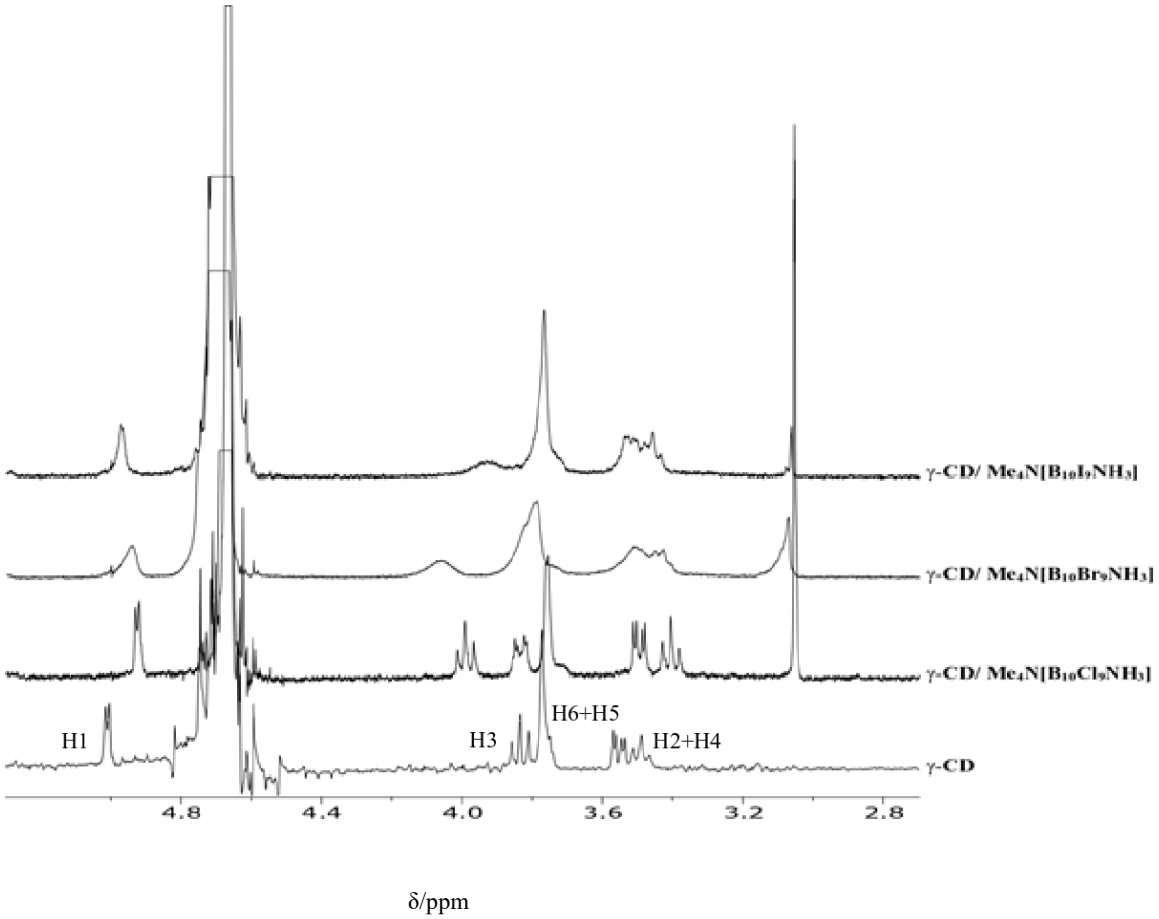

Fig. S11 ^{1}H NMR spectra of γ-CD with $Me_4N[B_{10}X_9NH_3]$ (X= Cl, Br, I) derivatives in D_2O

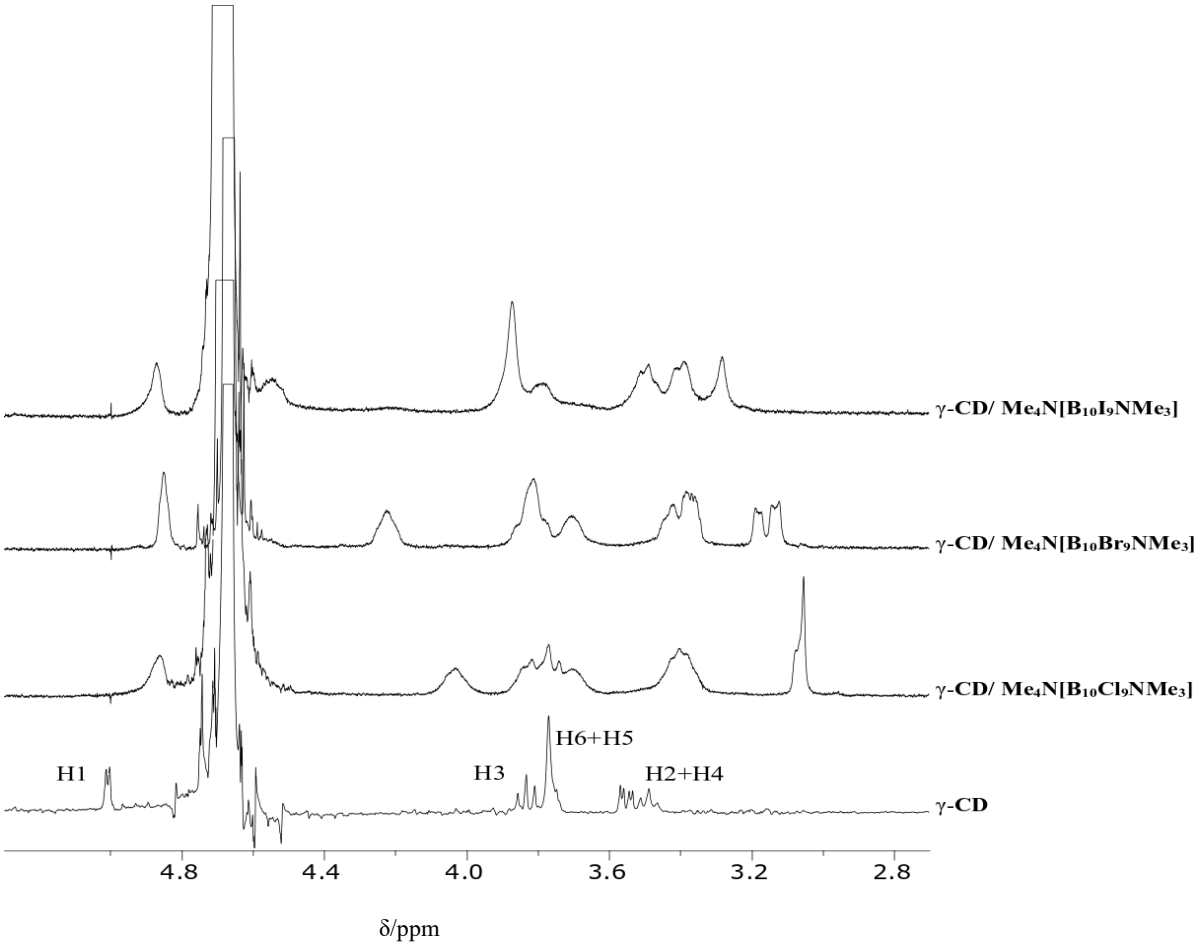

Fig. S12 ^{1}H NMR spectra of γ-CD with $Me_4N[B_{10}X_9NMe_3]$ derivatives (X= Cl, Br, I) in D_2O

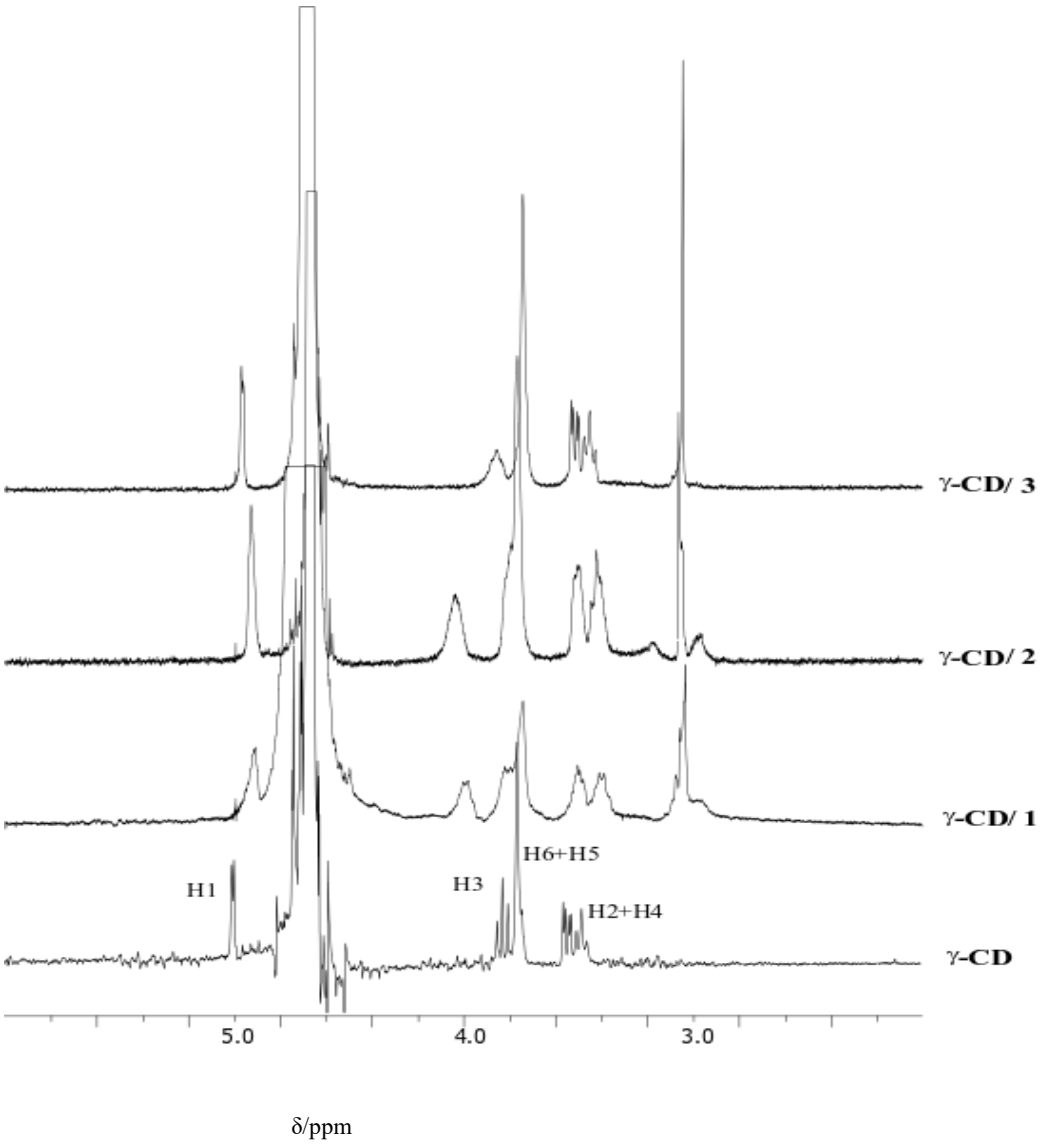

Fig. S13 ^{1}H NMR spectra of γ-CD with $Me_4N[B_{10}X_9NH_2CH_2CH(OH)CH_2NHBu]$, **1-3** (X= Cl, Br, I) derivatives in D_2O

- **NMR spectra of nonahalogenated 2-(propyleneoxide)ammonio-decaborate derivatives**

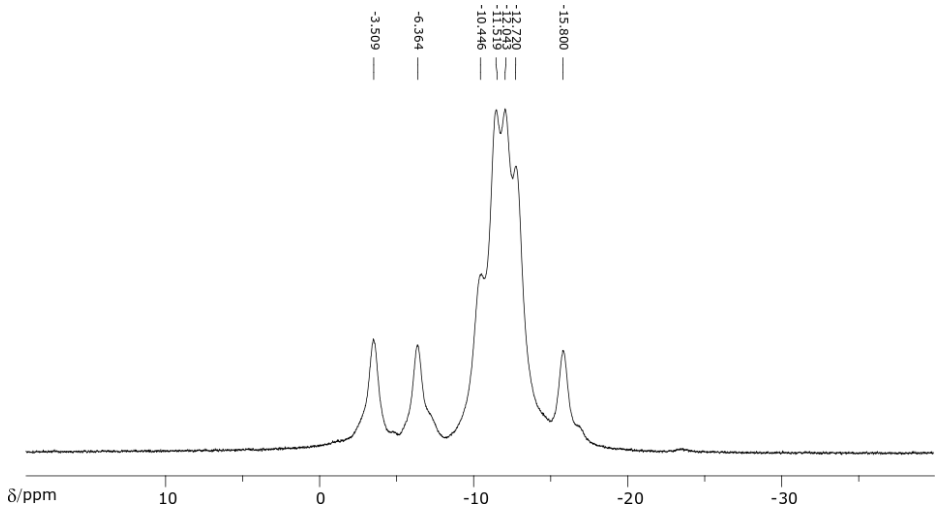

Fig. S14a ^{11}B NMR of compound **I**$^{-}$

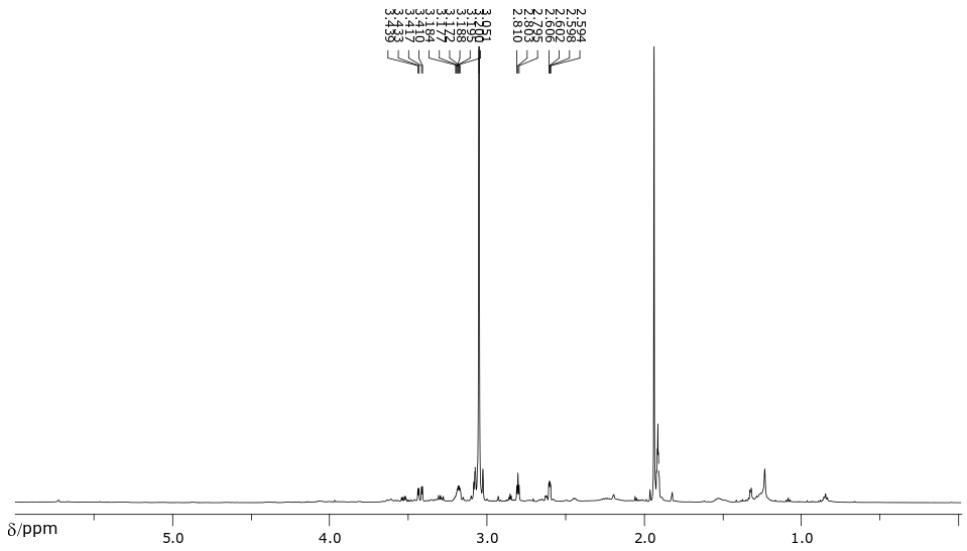

Fig. S14b ^{1}H NMR of compound **I**$^{-}$

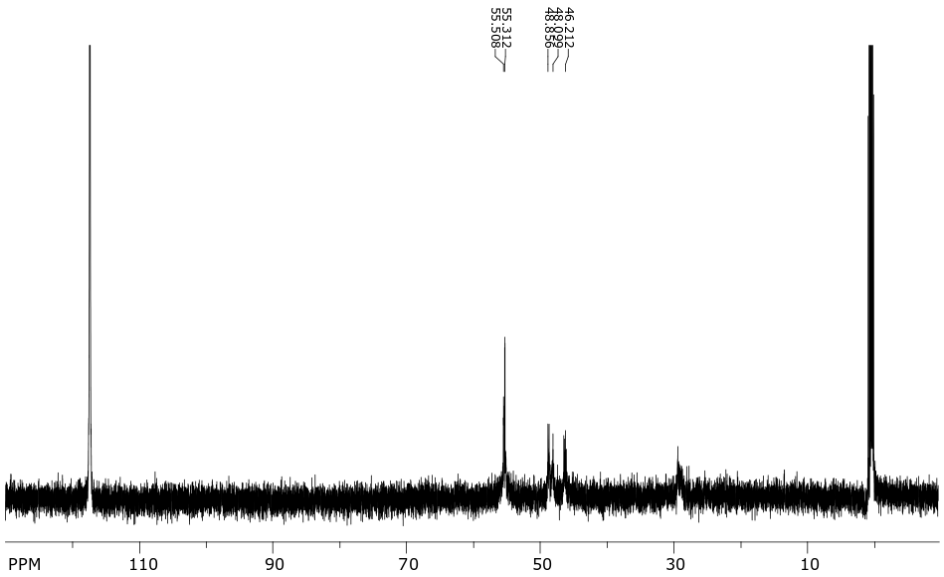

Fig. S14c ^{13}C NMR of compound **I**$^{-}$

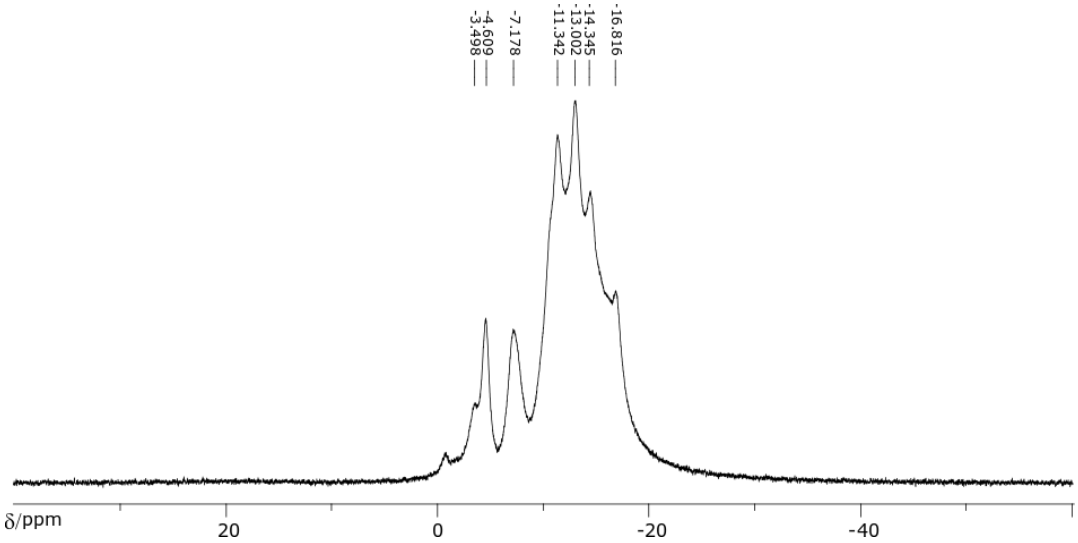

Fig. S15a ^{11}B NMR of compound **II**$^{-}$

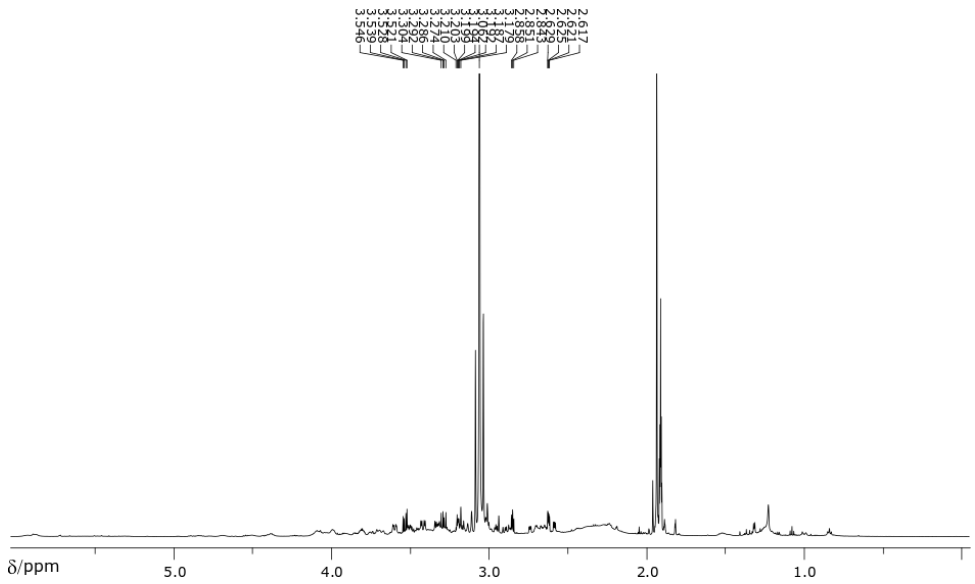

Fig. S15b ^{1}H NMR of compound **II**$^{-}$

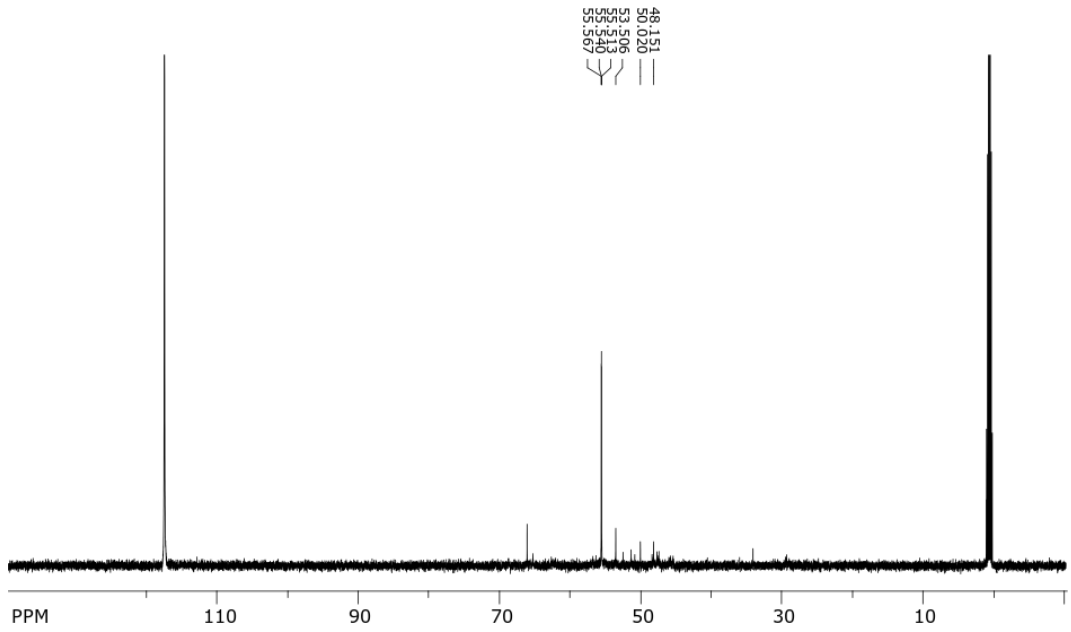

Fig. S15c ^{13}C NMR of compound **II**$^{-}$

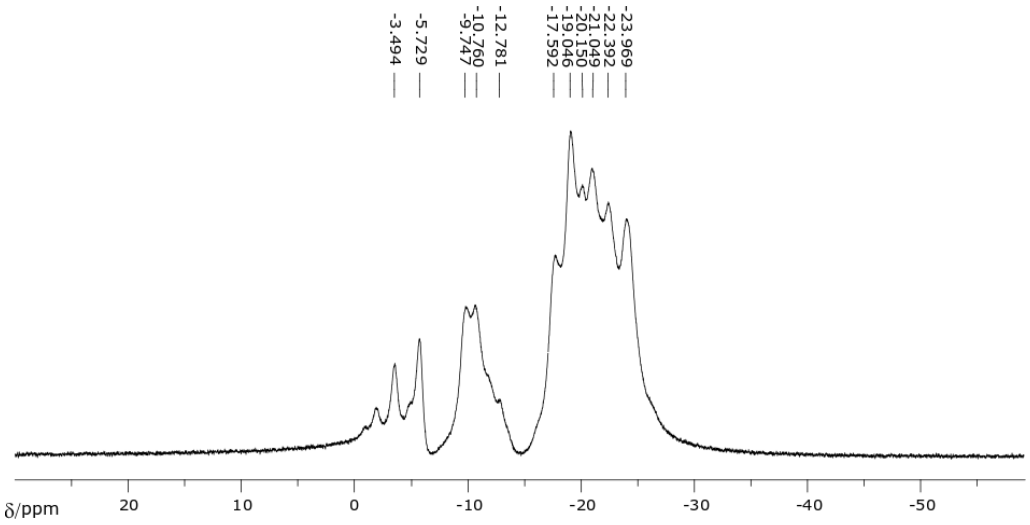

Fig. S16a ^{11}B NMR of compound **III**$^{-}$

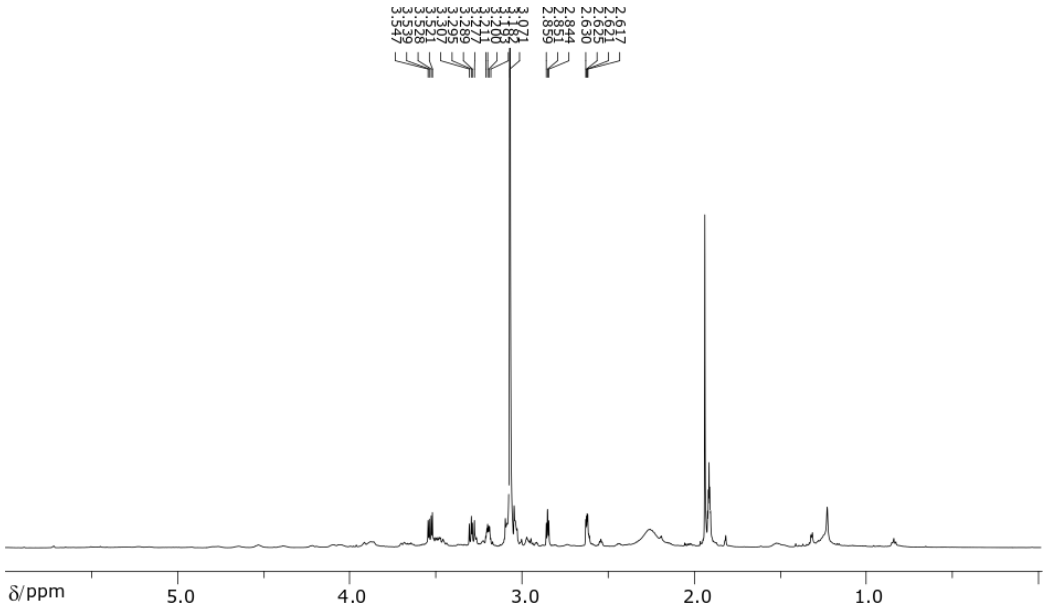

Fig. S16b ^{1}H NMR of compound **III**$^{-}$

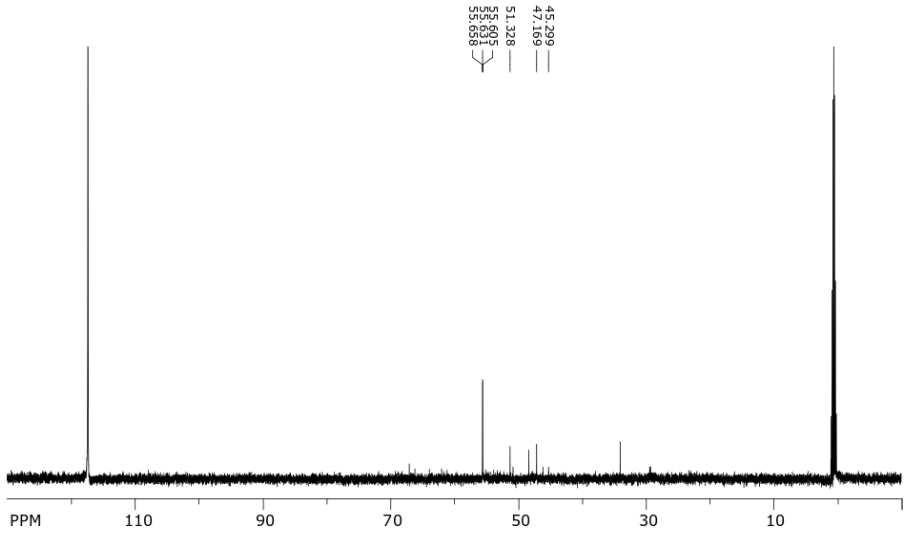

Fig. S16c ^{13}C NMR of compound **III**$^{-}$

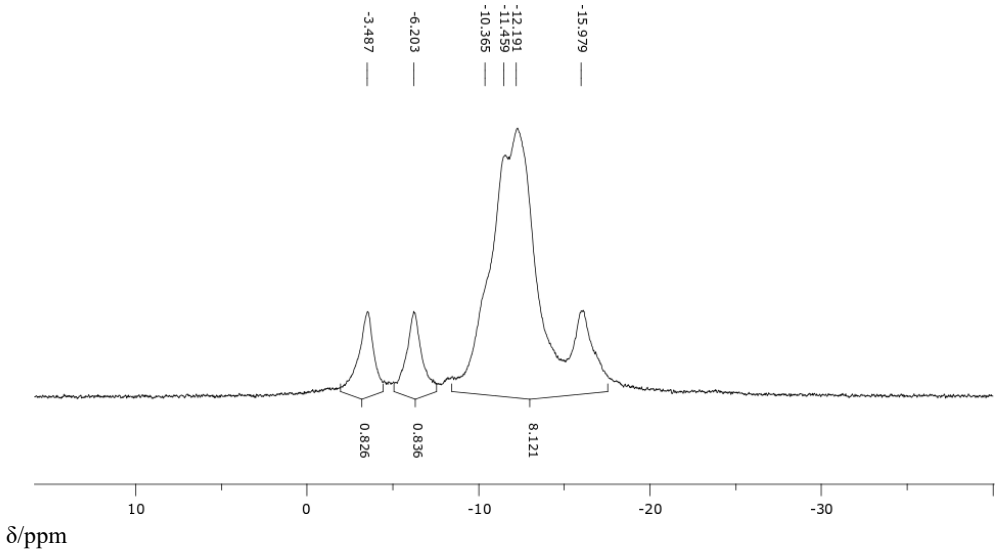

Fig. S17a ^{11}B NMR of compound **1**$^{-}$

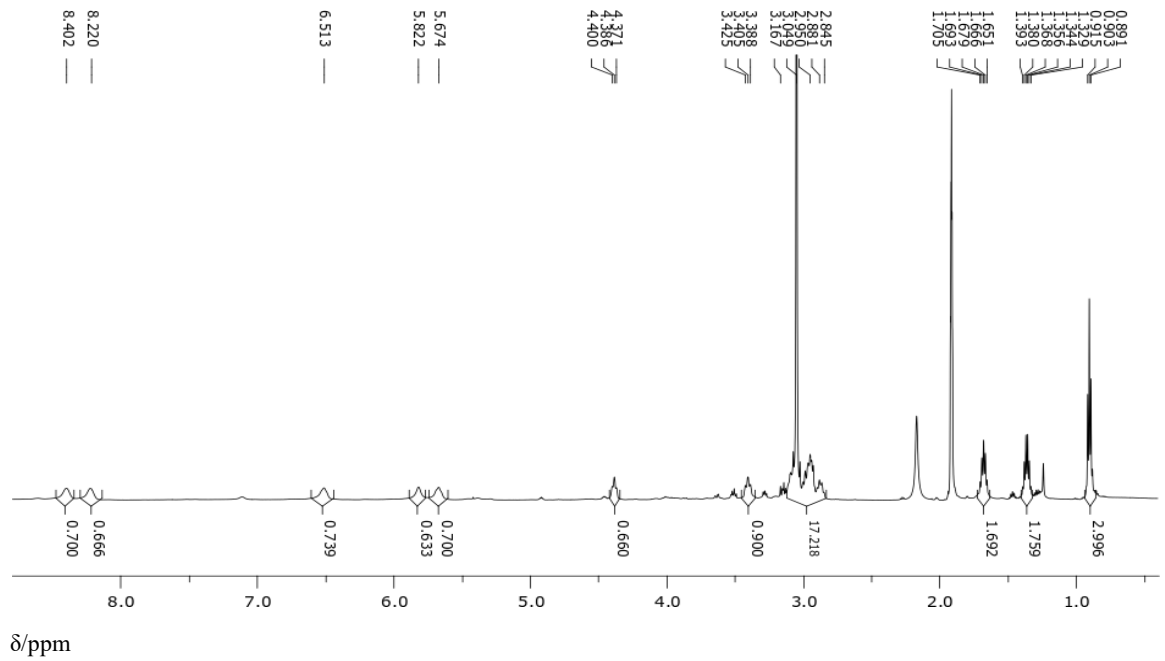

Fig. S17b ^{1}H NMR of compound **1**$^{-}$

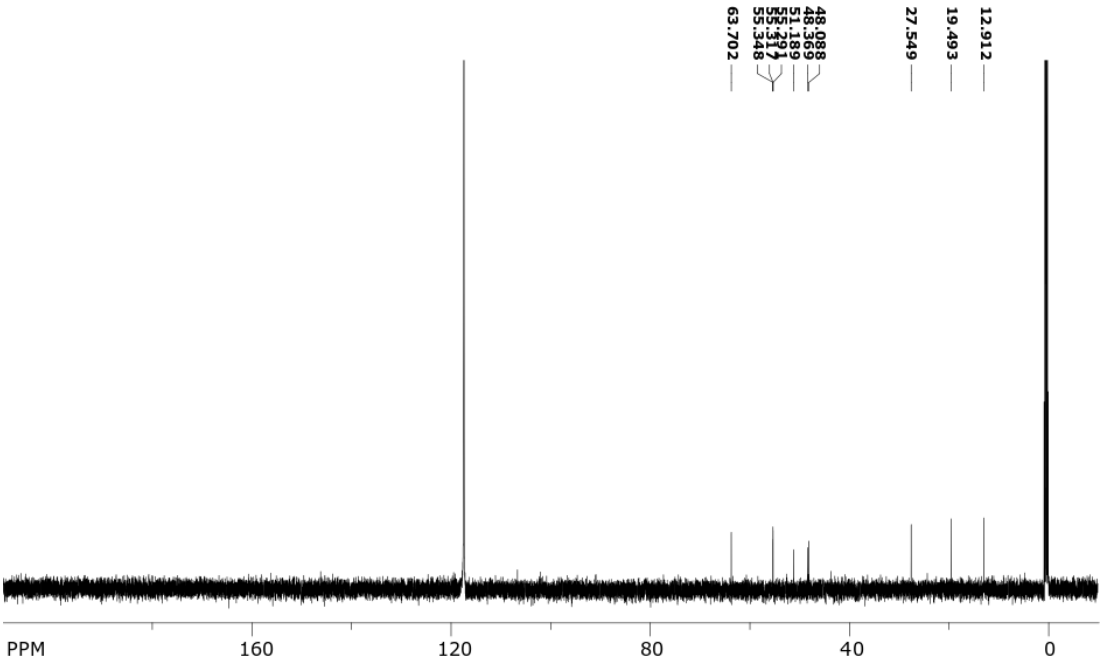

Fig. S17c ^{13}C NMR of compound **1**$^{-}$

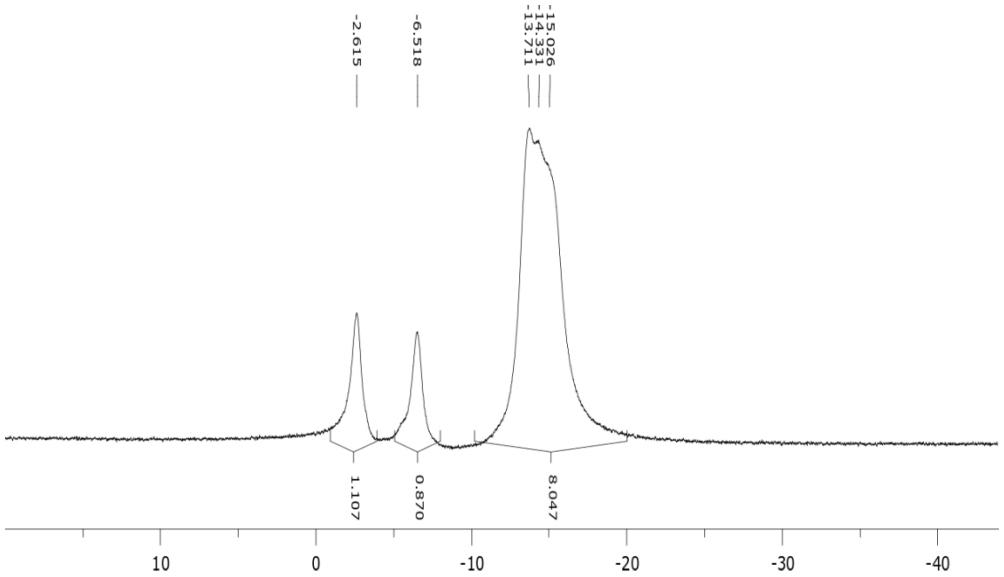

δ/ppm

Fig. S18a ^{11}B NMR of compound **2**$^{-}$

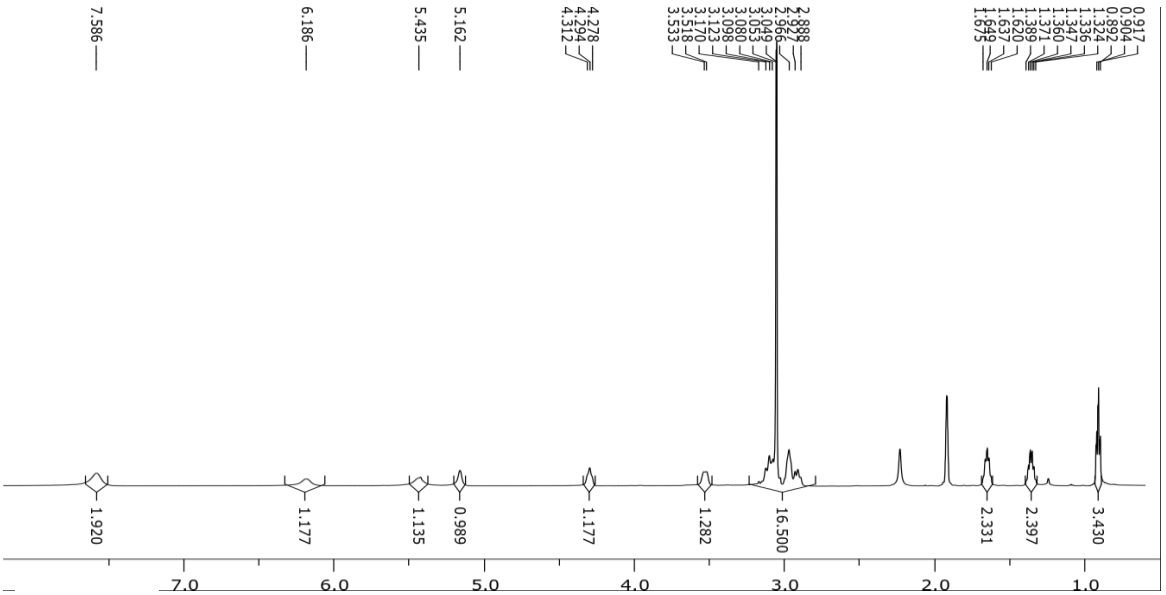

δ/ppm

Fig. S18b ^{1}H NMR of compound **2**$^{-}$

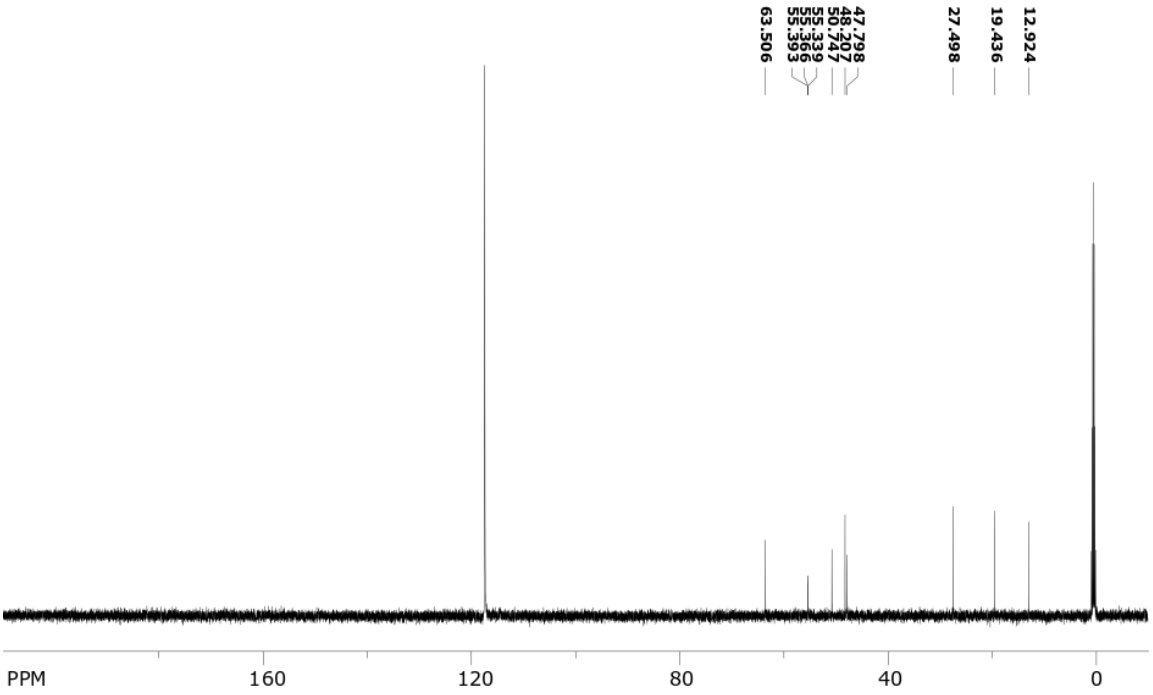

Fig. S18c ^{13}C NMR of compound **2**$^{-}$

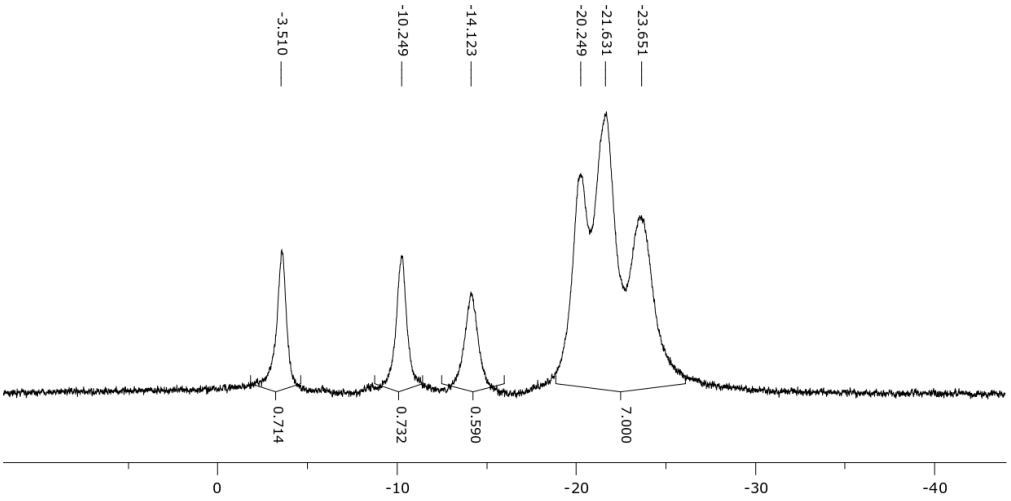

δ/ppm

Fig. S19a ^{11}B NMR of compound **3**$^{-}$

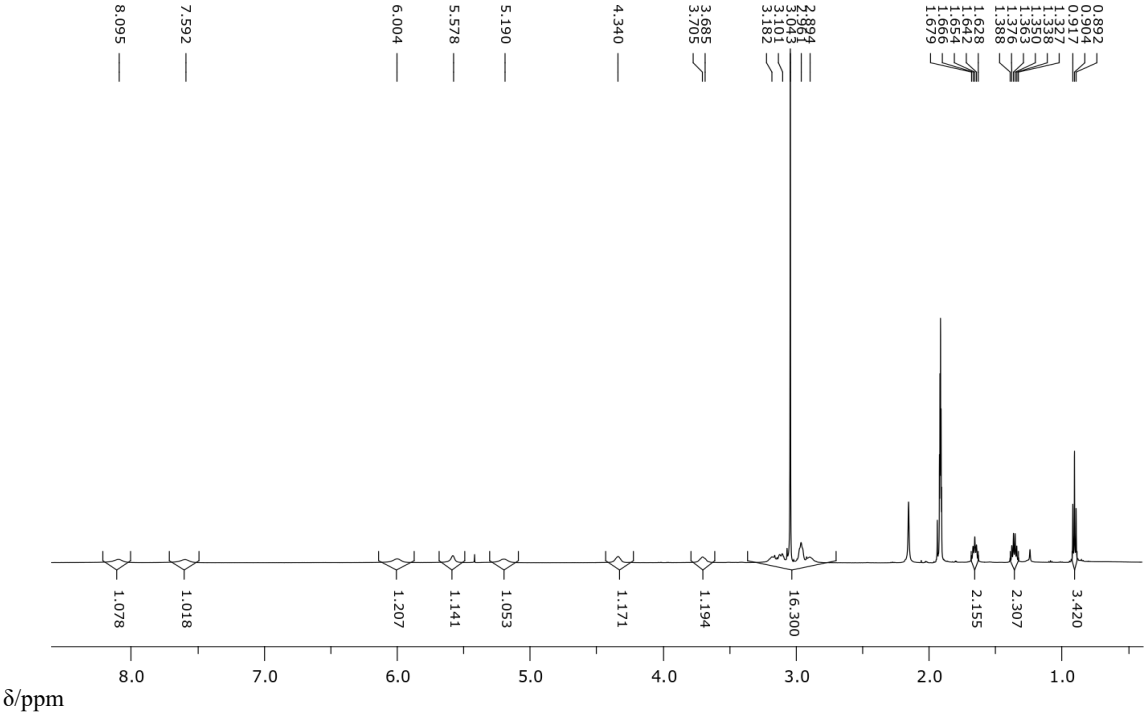

Fig. S19b ^{1}H NMR of compound **3**$^{-}$

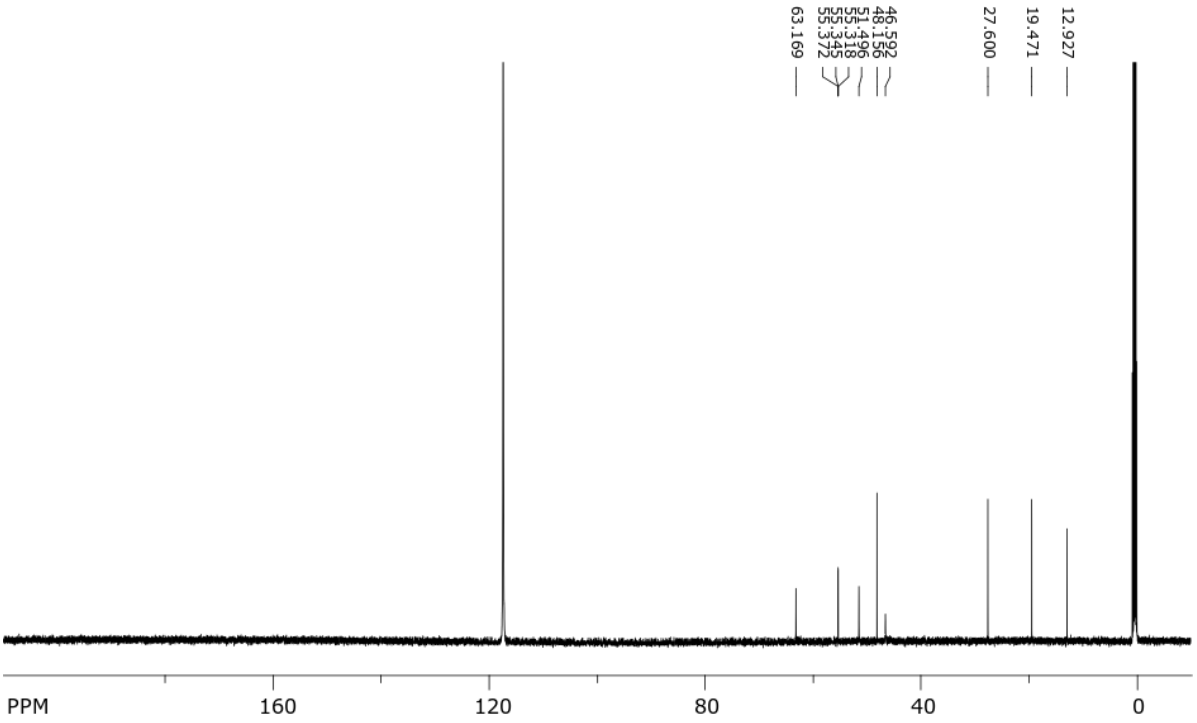

Fig. S19c ^{13}C NMR of compound **3**$^{-}$

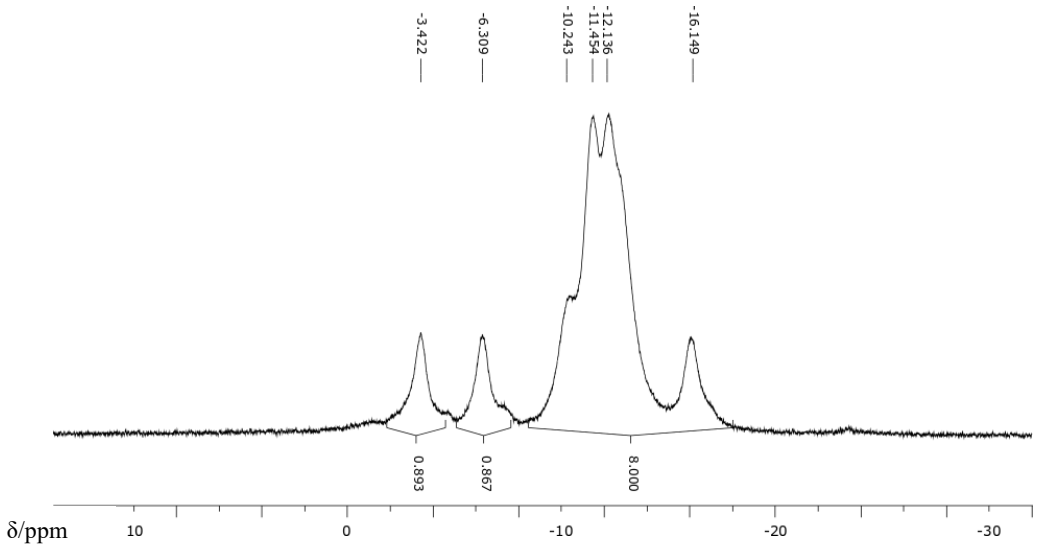

Fig. S20a ^{11}B NMR of compound **4**$^{-}$

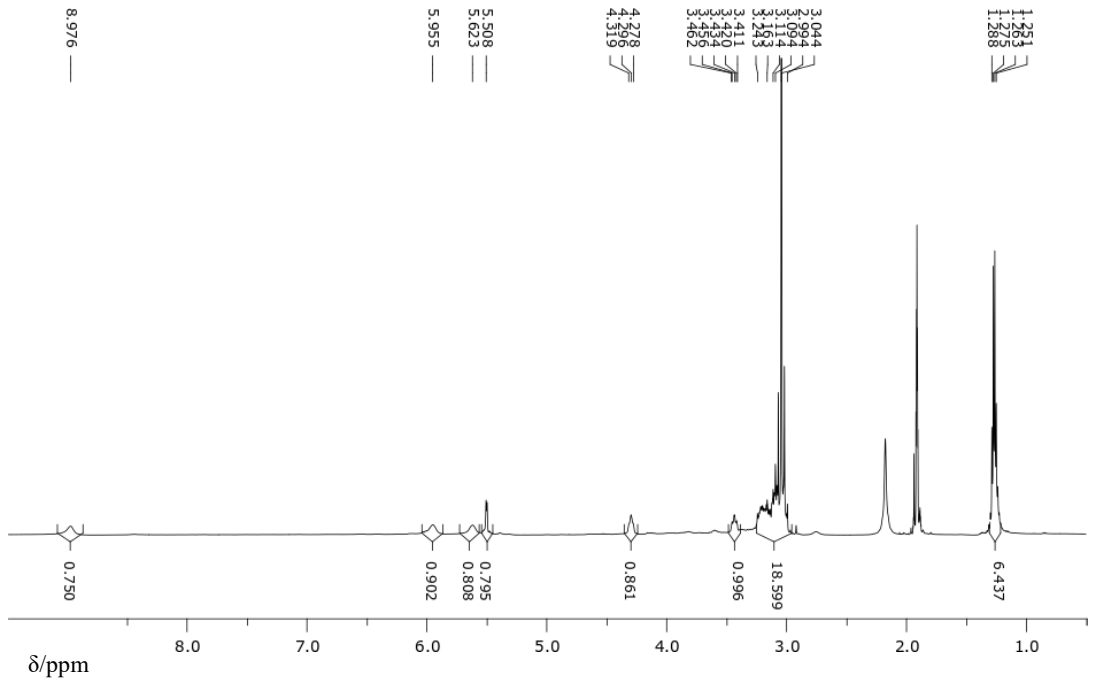

Fig. S20b ^{1}H NMR of compound **4**$^{-}$

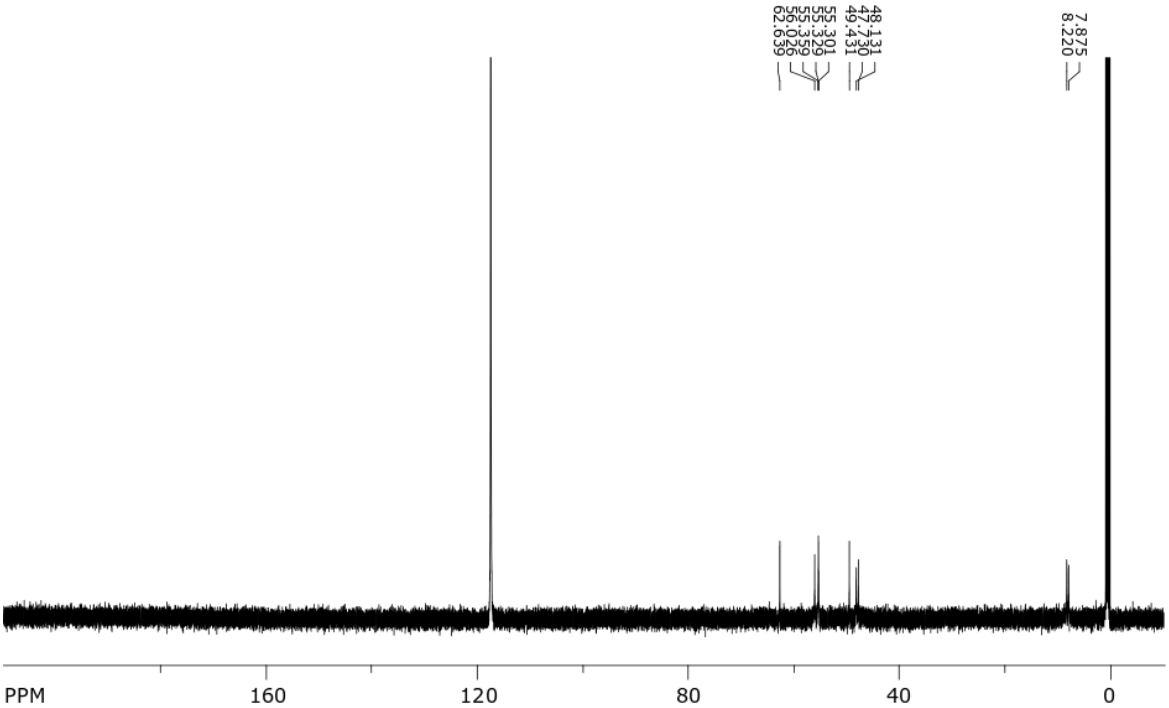

Fig. S20c ^{13}C NMR of compound **4**$^{-}$

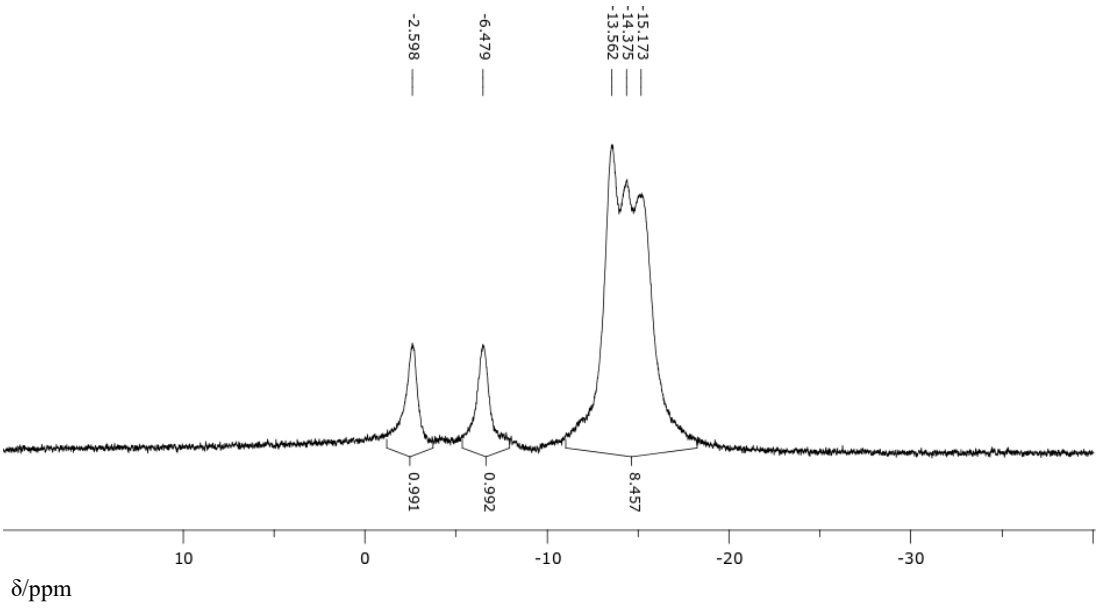

Fig. S21a ^{11}B NMR of compound **5**$^{-}$

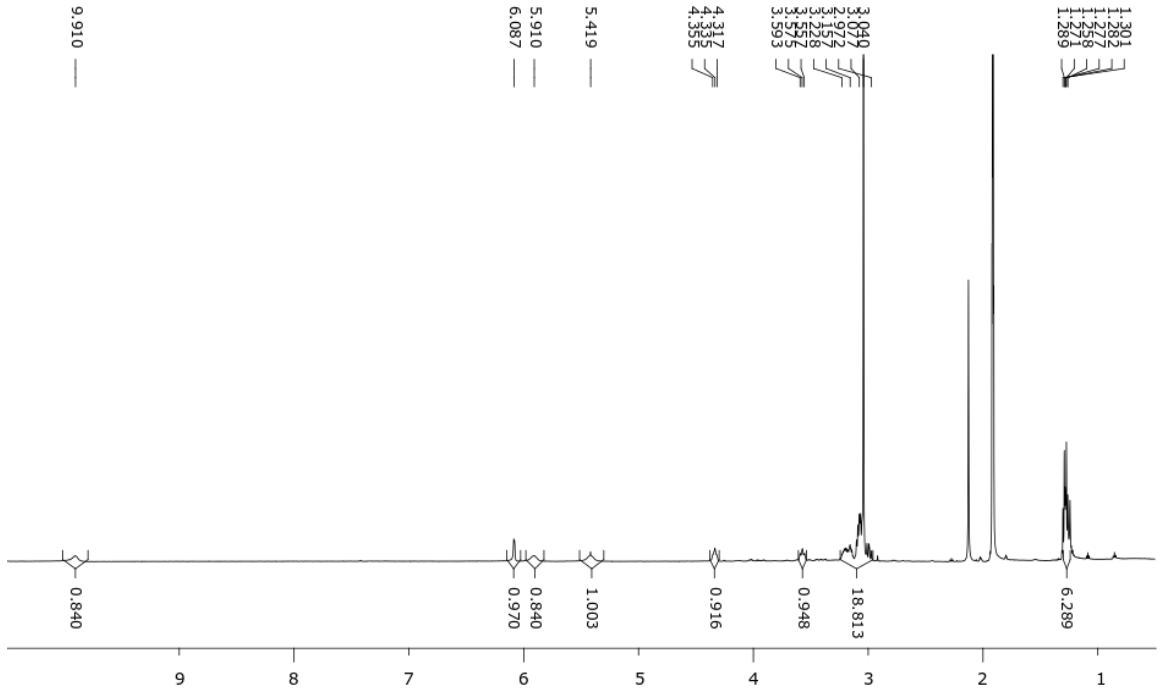

Fig. S21b ^{1}H NMR of compound **5**$^{-}$

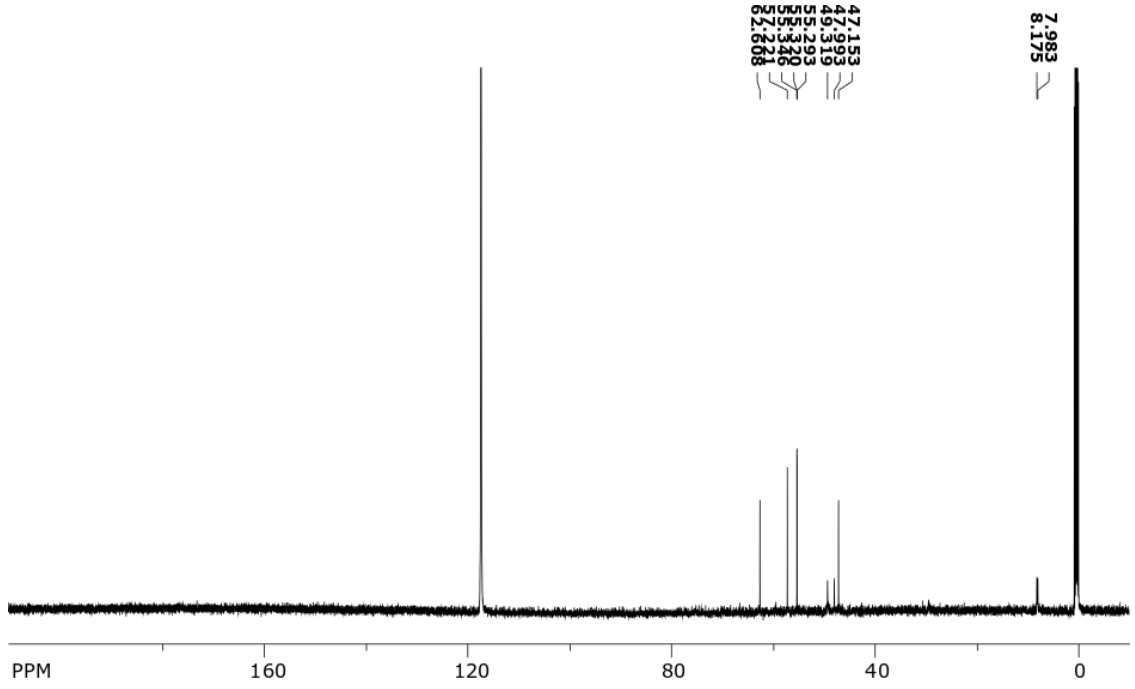

Fig. S21c ^{13}C NMR of compound **5**$^{-}$

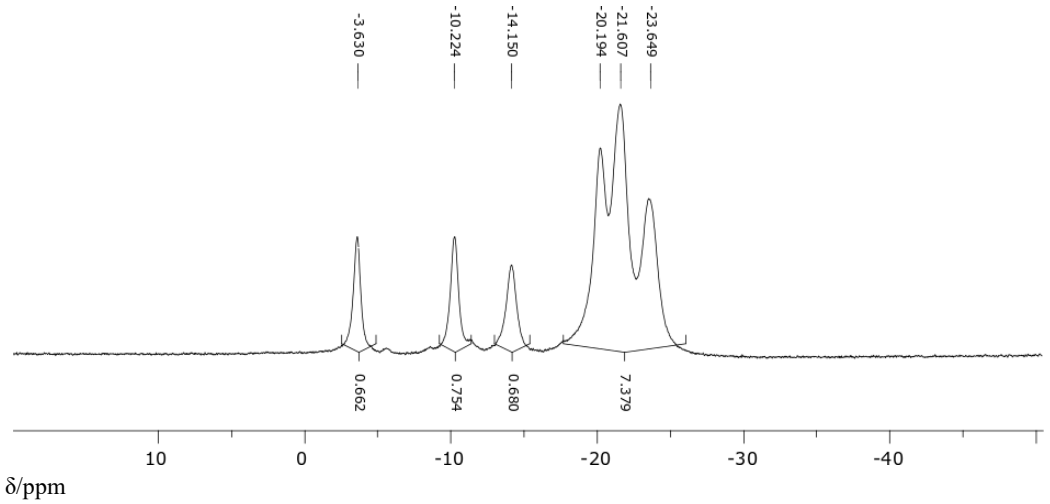

Fig. S22a ^{11}B NMR of compound **6**$^{-}$

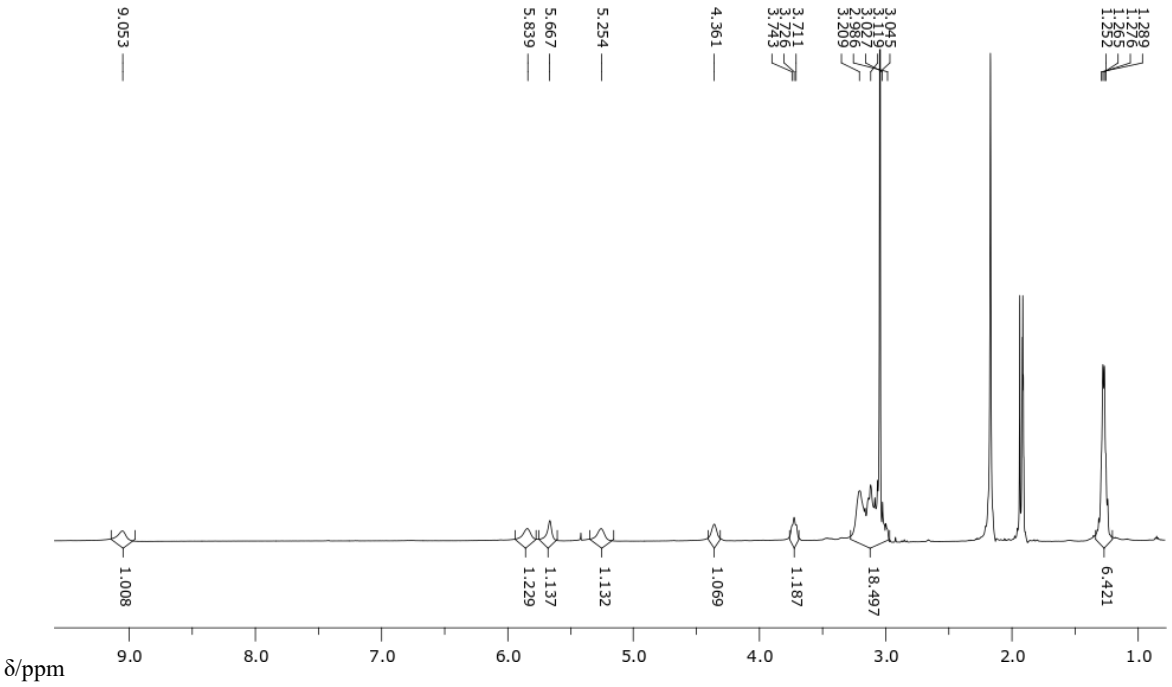

Fig. S22b ^{1}H NMR of compound **6**$^{-}$

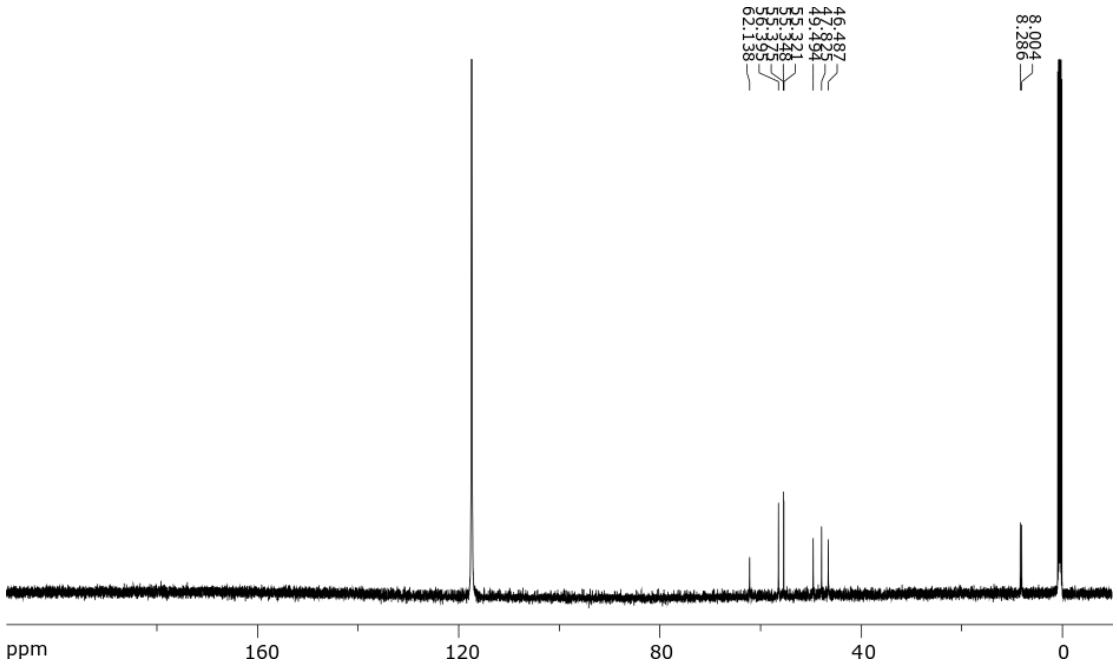

Fig. S22c ^{13}C NMR of compound **6**$^{-}$

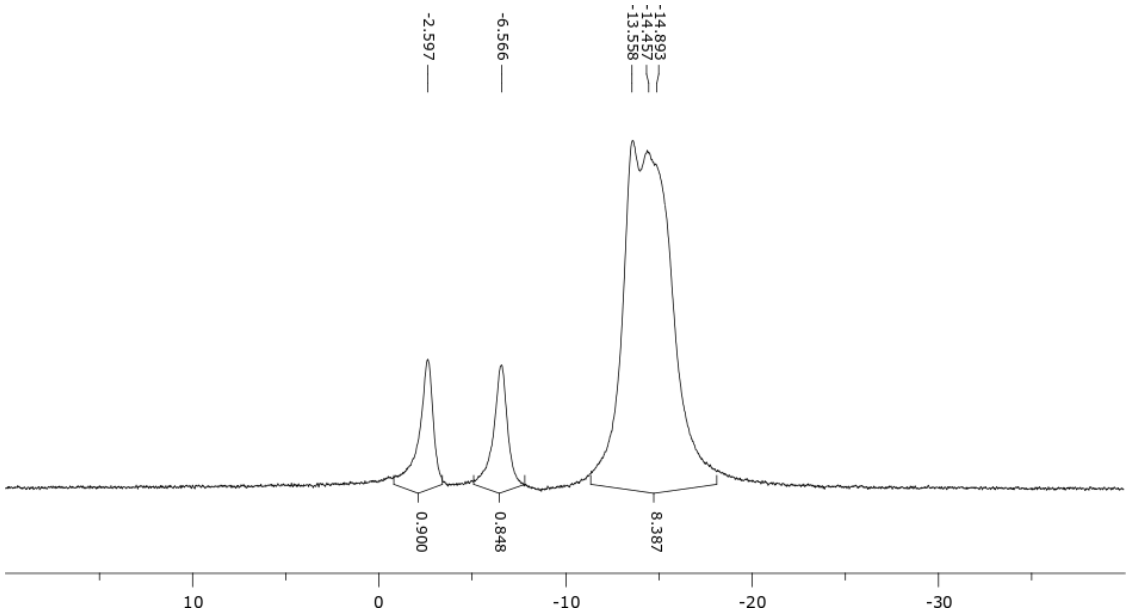

Fig. S23a ^{11}B NMR of compound **7**$^{-}$

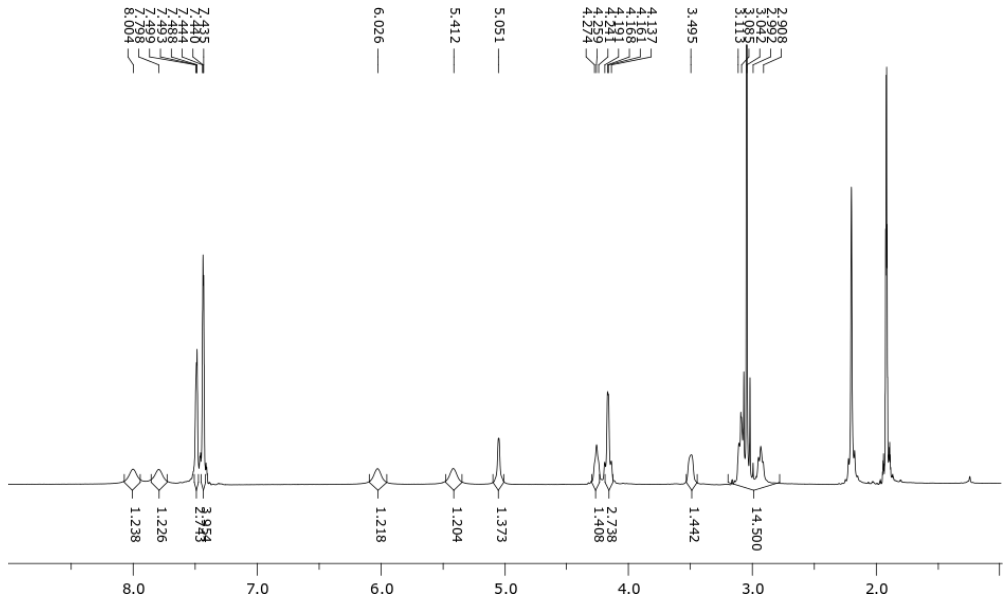

δ/ppm

Fig. S23b ^{1}H NMR of compound **7**$^{-}$

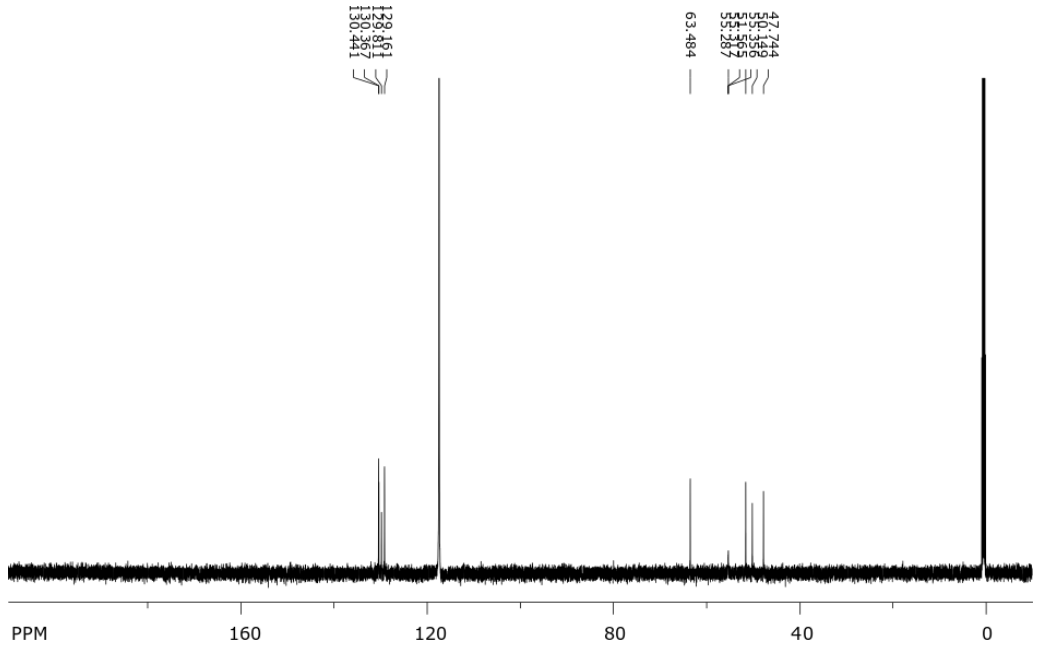

Fig. S23c ^{13}C NMR of compound **7**$^{-}$

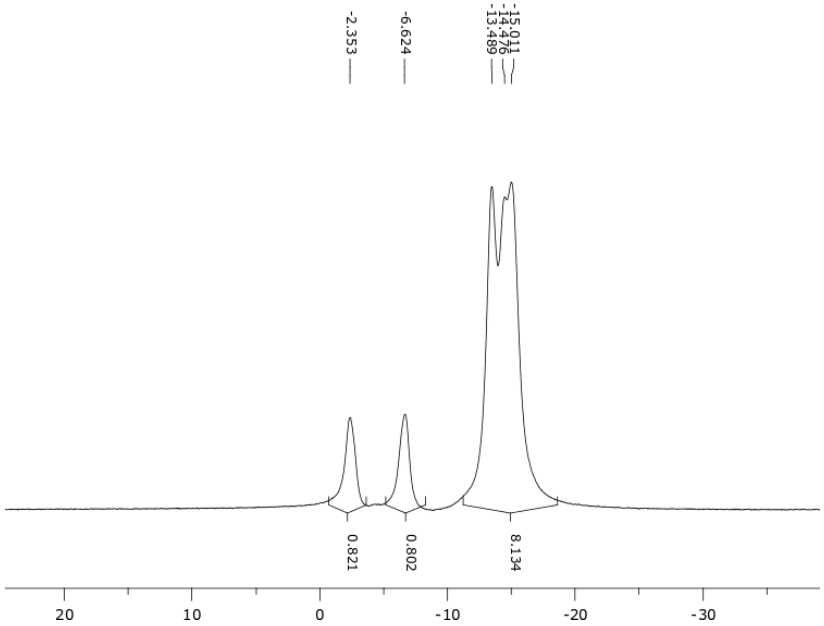

Fig. S24a ^{11}B NMR of compound **8**$^{-}$

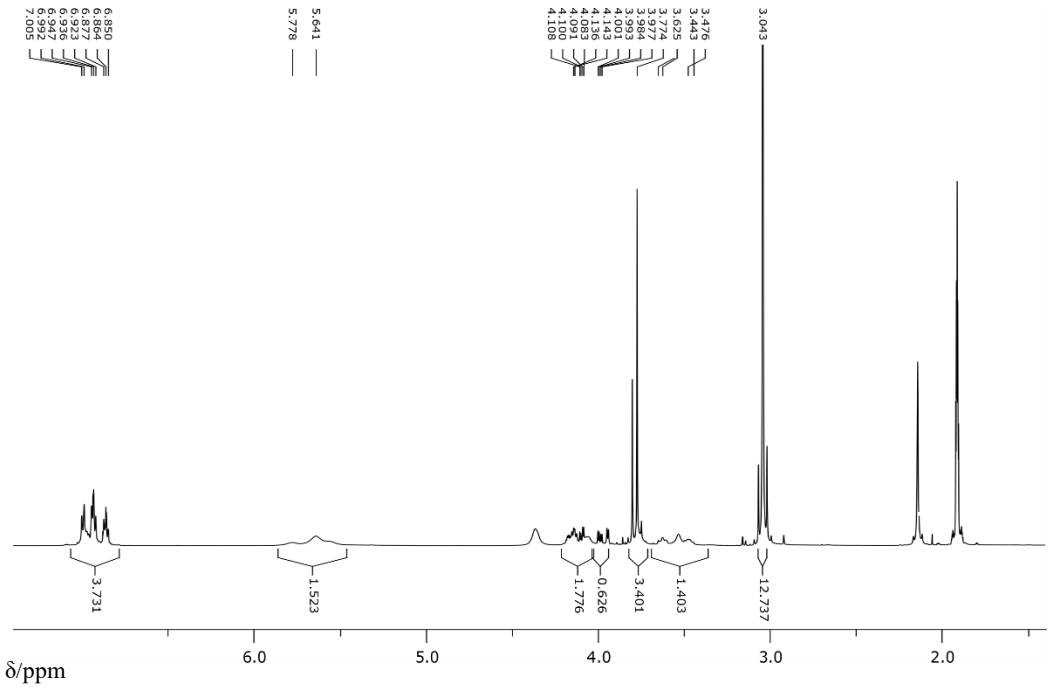

Fig. S24b ^{1}H NMR of compound **8**$^{-}$

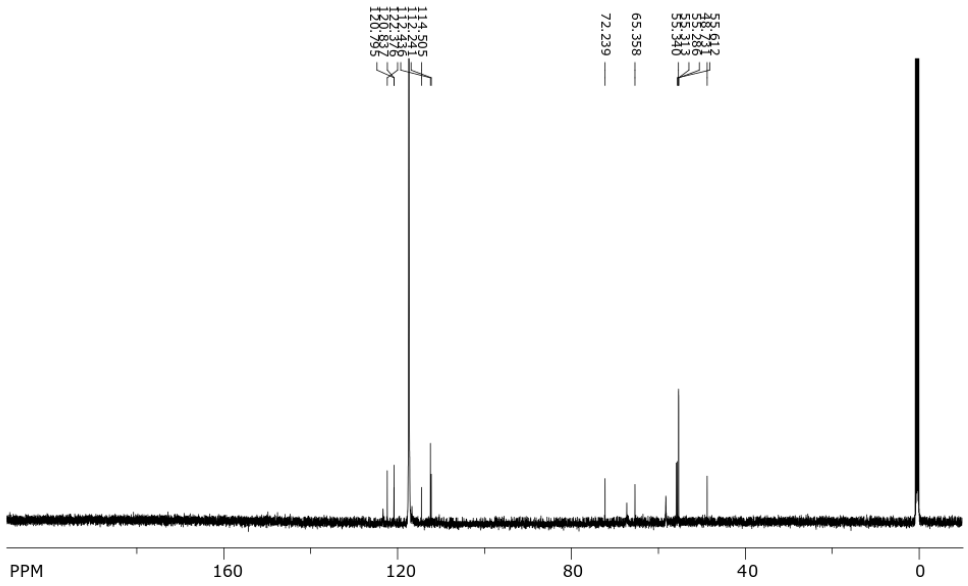

Fig. S24c ^{13}C NMR of compound **8**$^{-}$

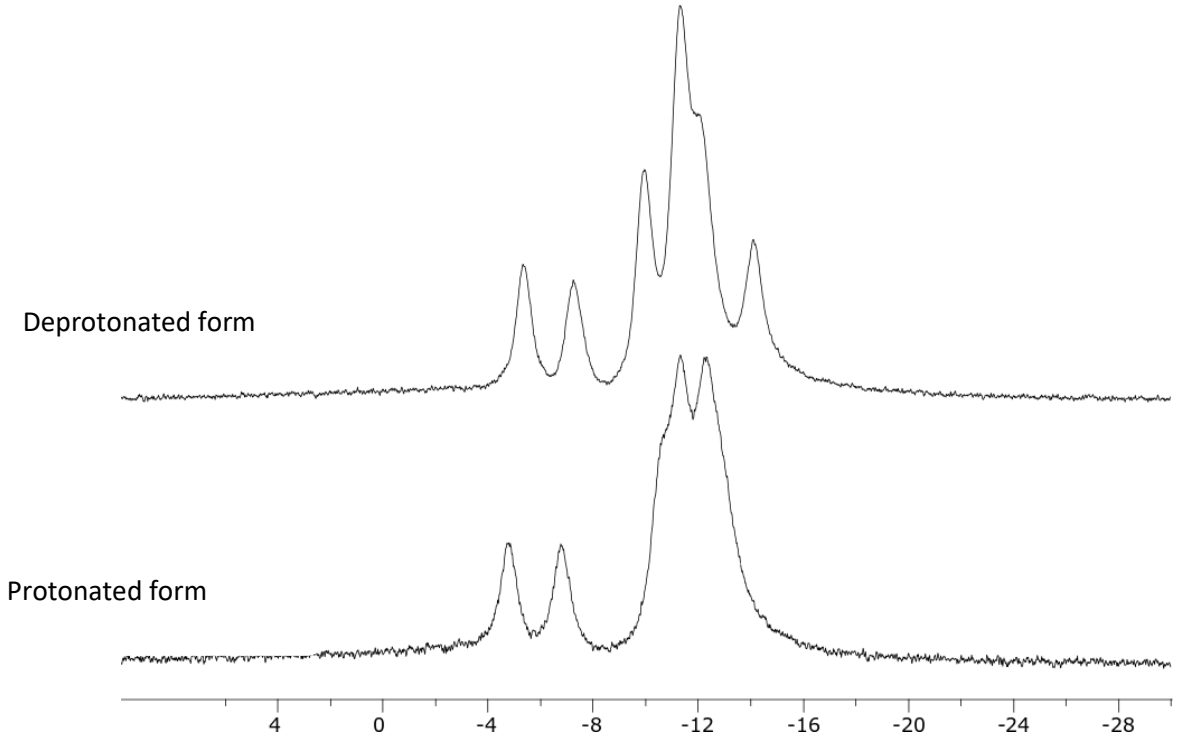

Fig. S25 ^{11}B NMR spectra of Me_4N $[B_{10}Cl_9NH_2CH_2CH(OH)CH_2NH(CH_2)_3CH_3]$ (**1**$^{-}$) in protonated and deprotonated form after addition of KOH in CD_3CN

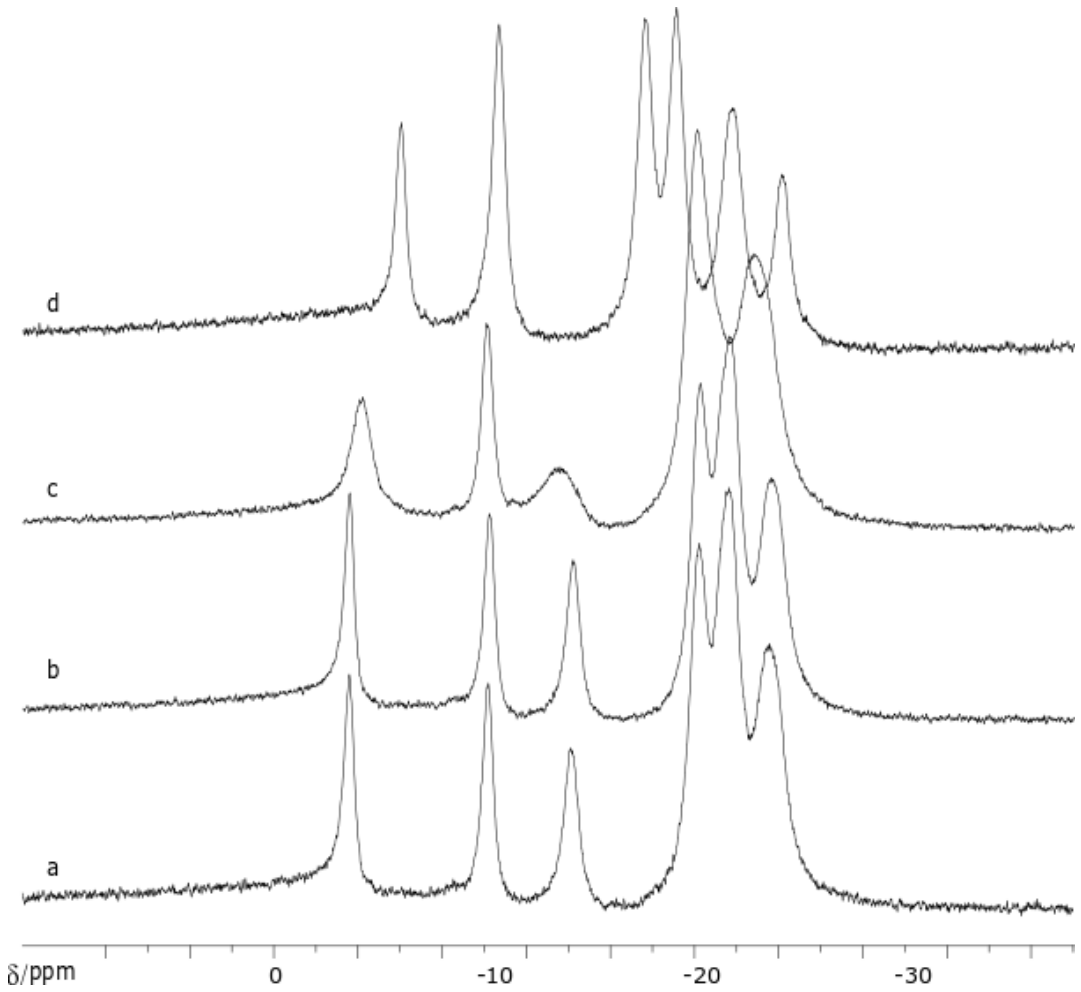

Fig. S26 ^{11}B NMR spectra of a) Me_4N $[B_{10}I_9NH_2CH_2CH(OH)CH_2NH(CH_2)_3CH_3]$, (**3**$^-$), b) after adding HCl (3M), c) after neutralizing the solution with equivalent portion of 3M KOH (d) after making it alkaline with an excess of 3M KOH

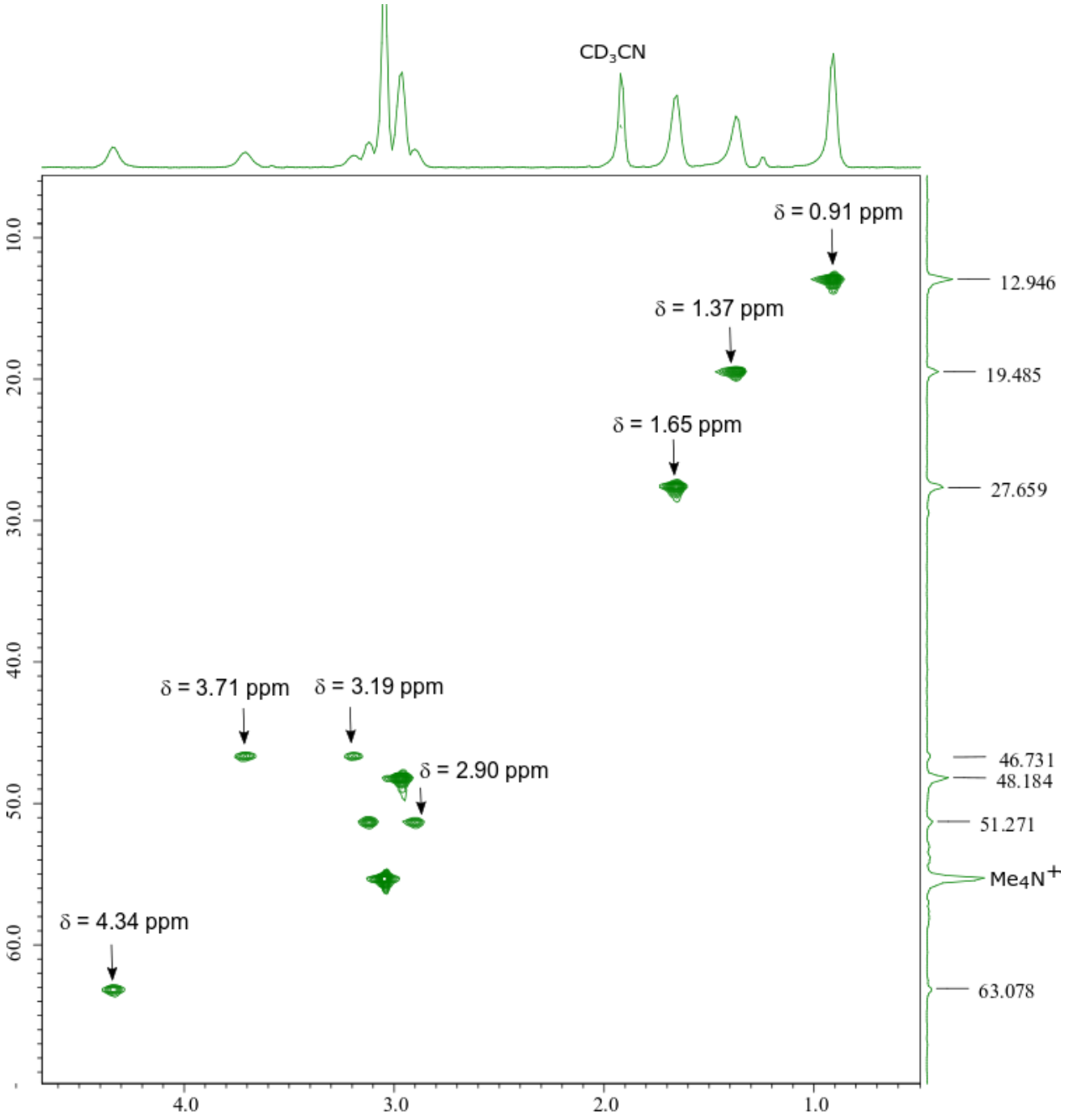

Fig. S27a ^{1}H-^{13}C HSQC of $Me_4N[B_{10}I_9NH_2CH_2CH(OH)CH_2NH(CH_2)_3CH_3]$, (**3**$^-$).

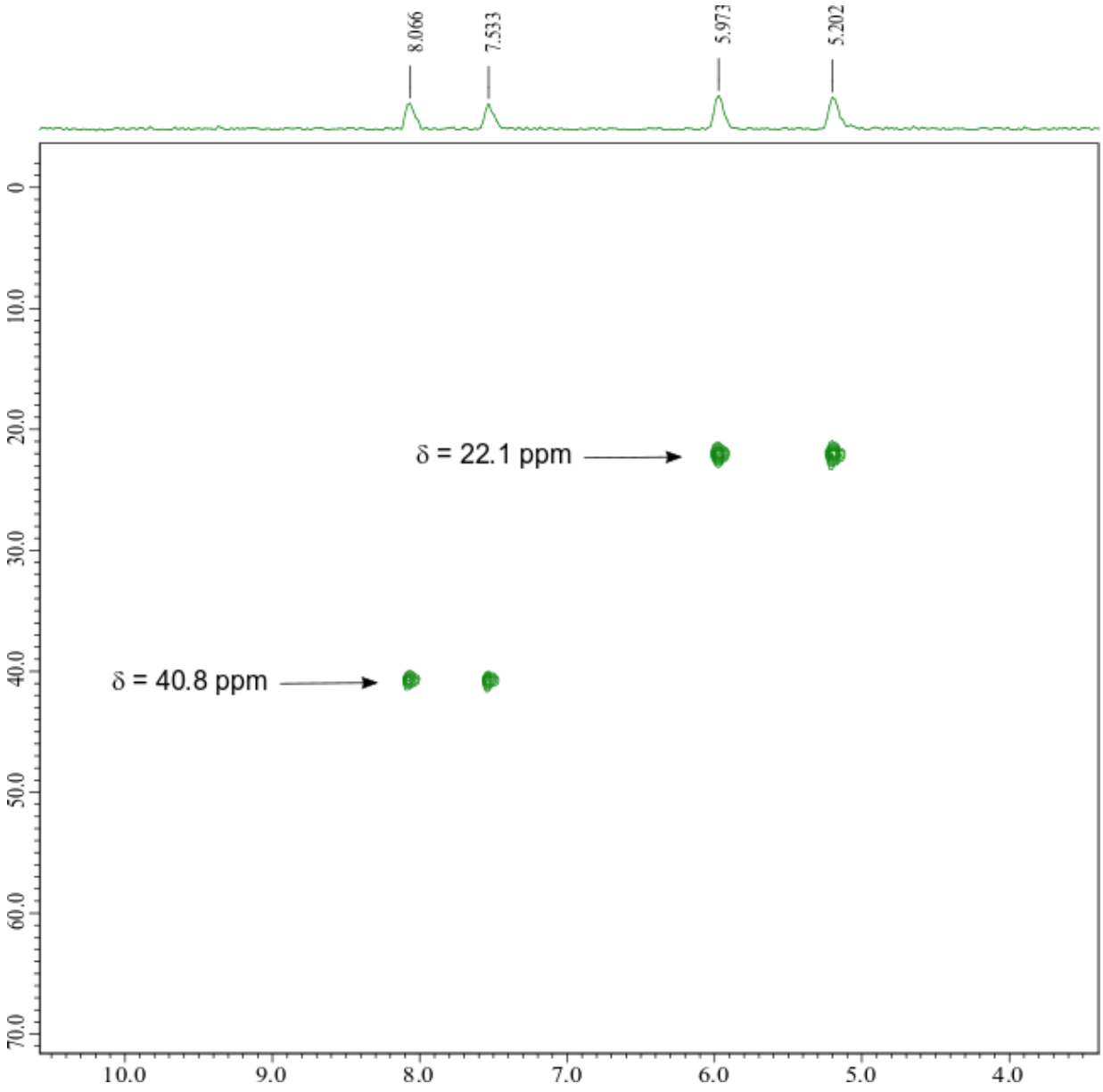

Fig. S27b ^{1}H-^{15}N HSQC of protonated $[B_{10}I_9NH_2CH_2CH(OH)CH_2NH_2(CH_2)_3CH_3]$, (**3**$^-$).

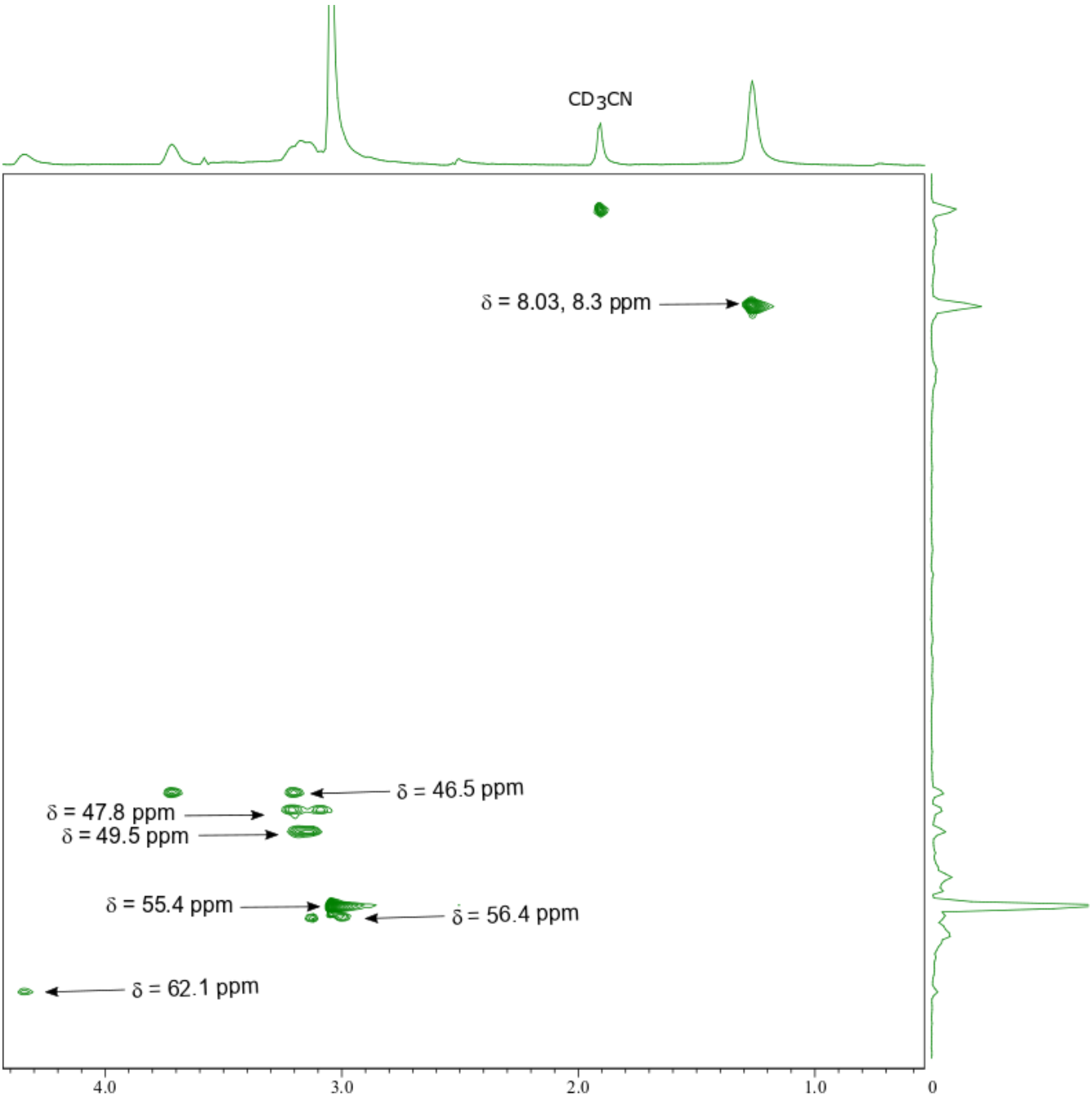

Fig. S28a ^{1}H-^{13}C HSQC of Me_4N $[B_{10}I_9NH_2CH_2CH(OH)CH_2N(CH_2CH_3)_2]$, (**6**$^-$).

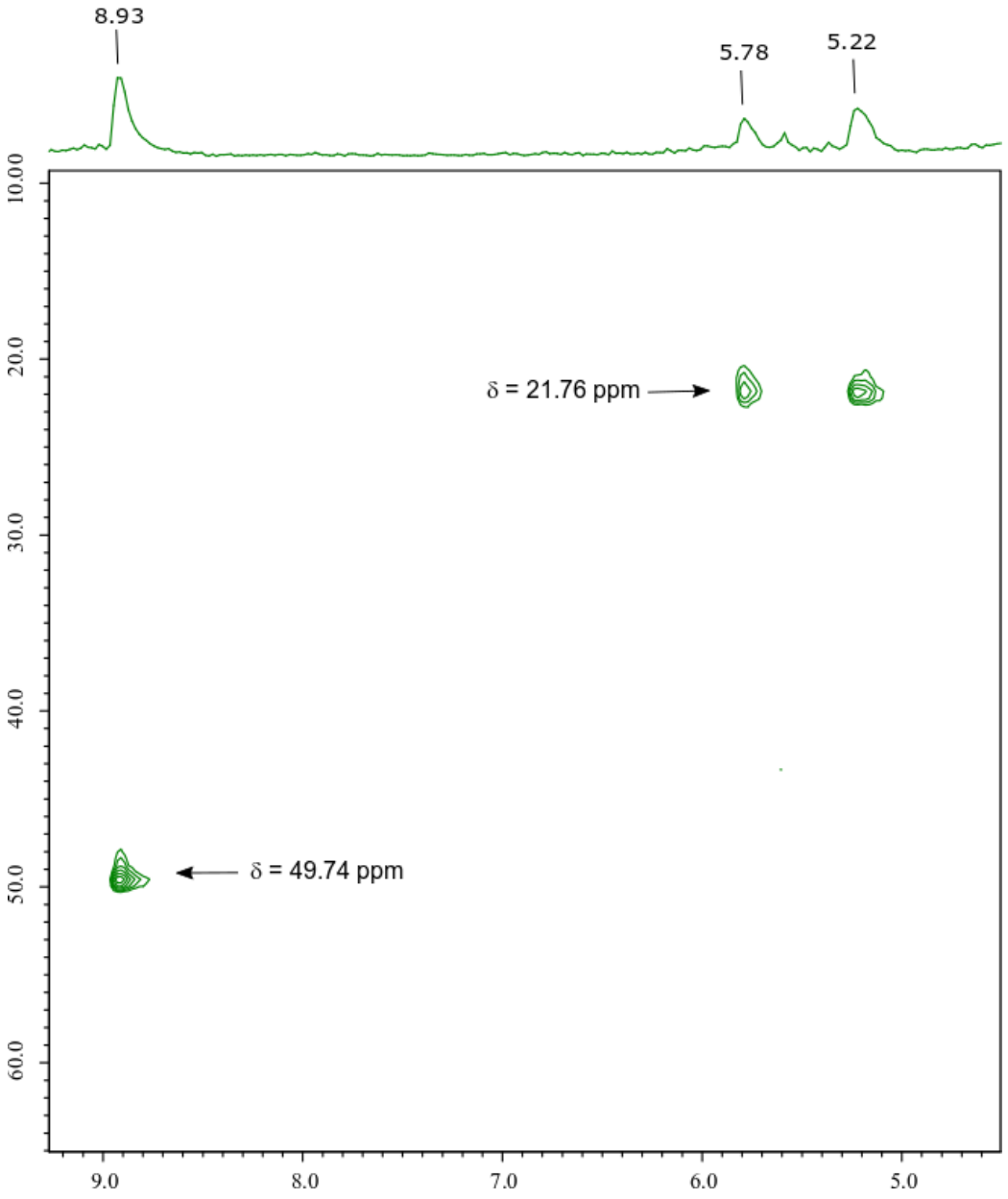

Fig. S28b ^{1}H-^{15}N HSQC of Me_4N $[B_{10}I_9NH_2CH_2CH(OH)CH_2N(CH_2CH_3)_2]$], (**6**$^{-}$).

6. ESI Mass Spectra

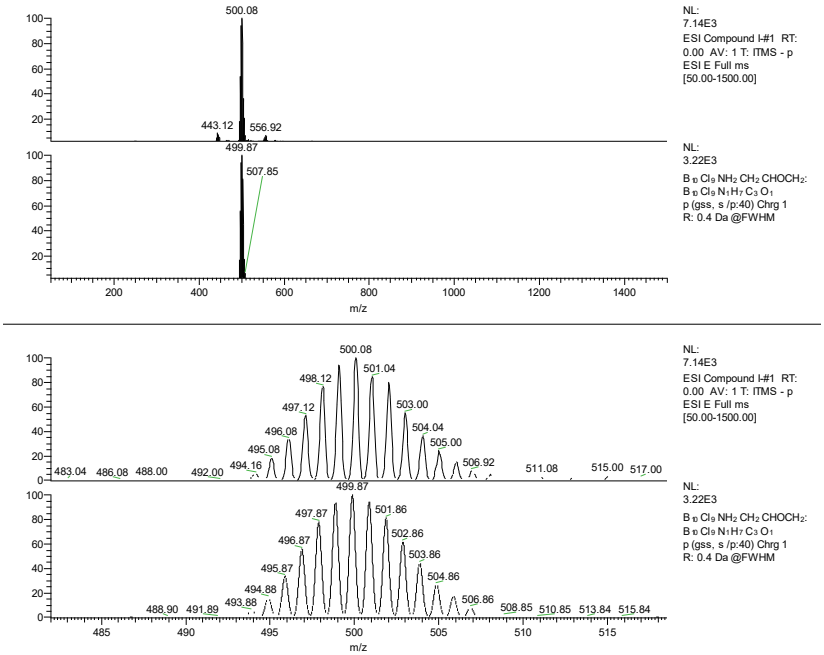

Fig. 29 Mass spectrum of **I**$^-$

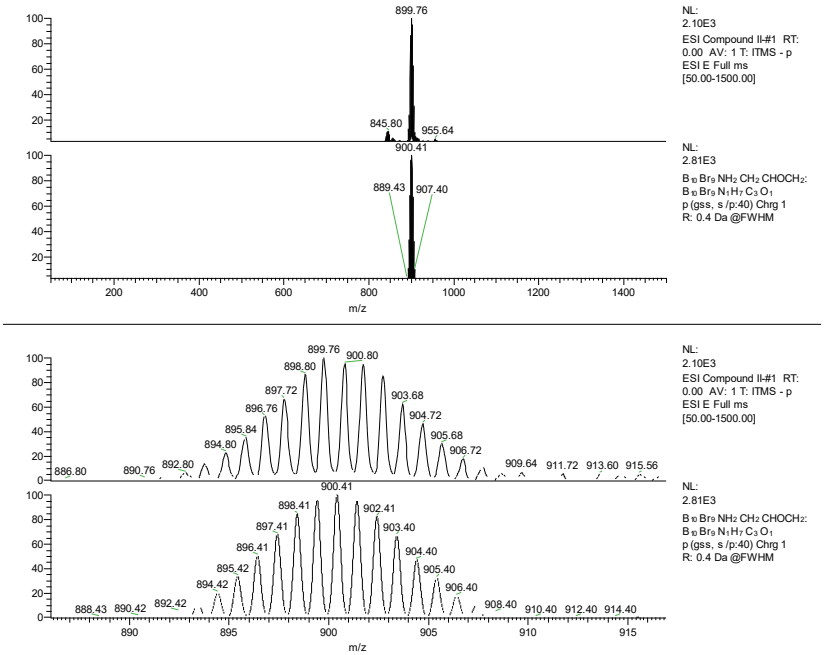

Fig. 30 Mass spectrum of **II**$^-$

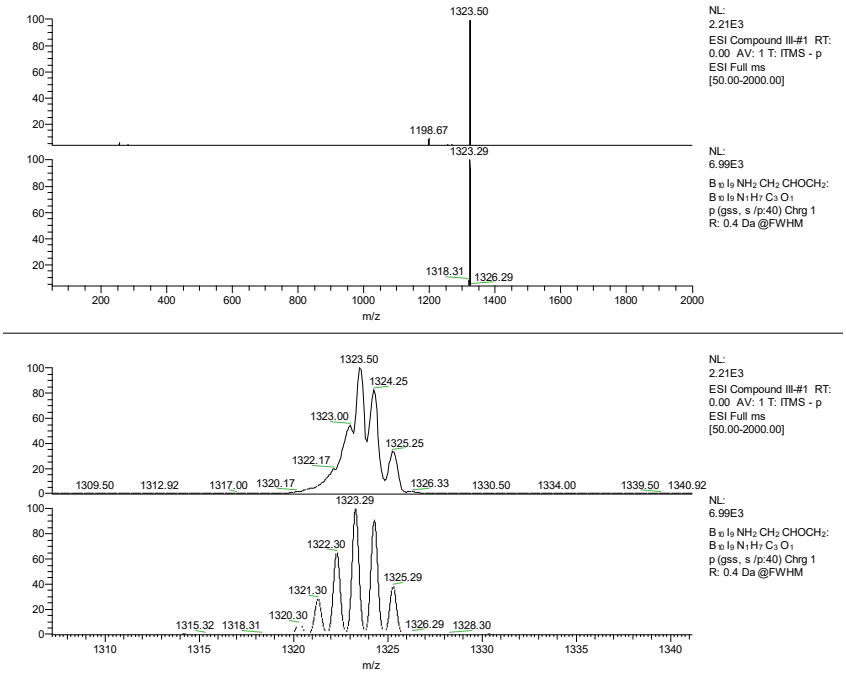

Fig. 31 Mass spectrum of **III**$^-$

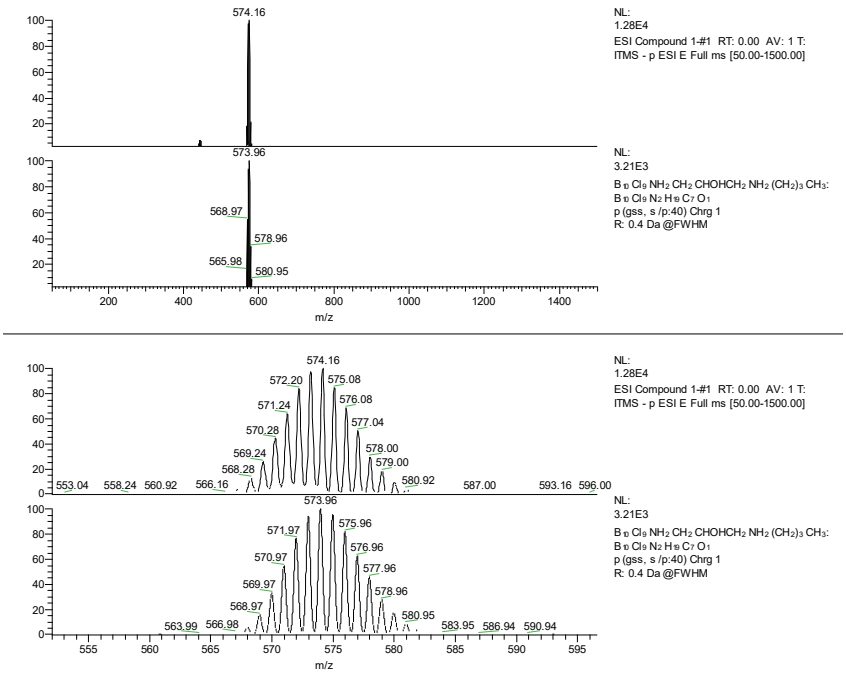

Fig. 32 Mass spectrum of **1**$^-$

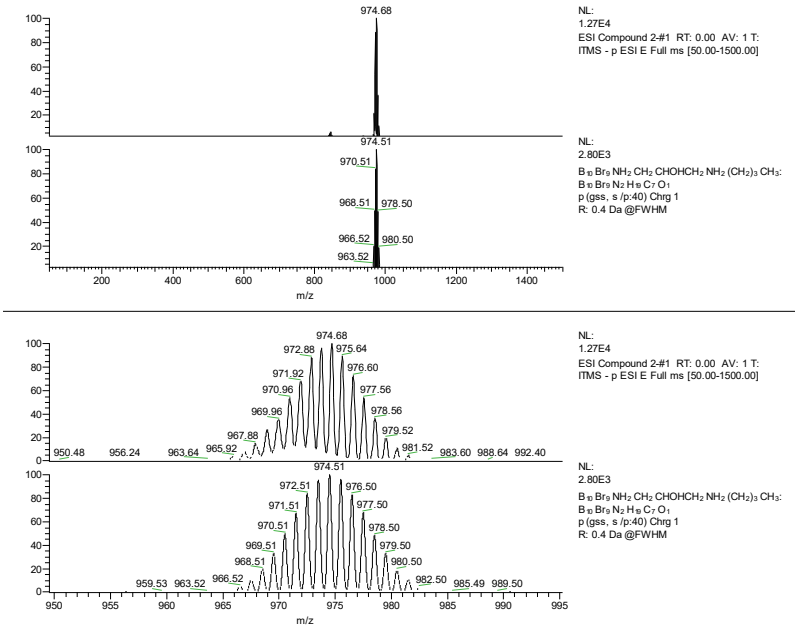

Fig. 33 Mass spectrum of **2**$^{-}$

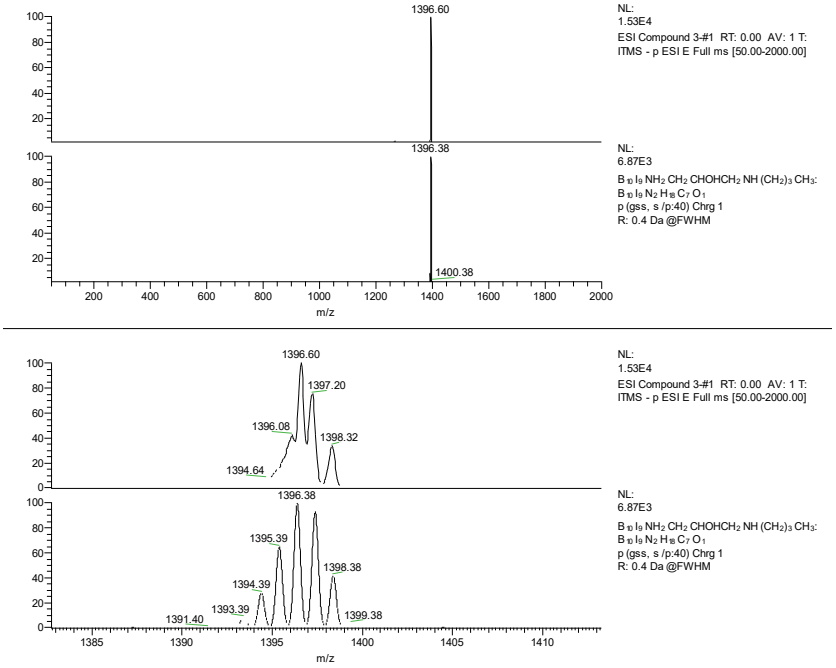

Fig. 34 Mass spectrum of **3**$^{-}$

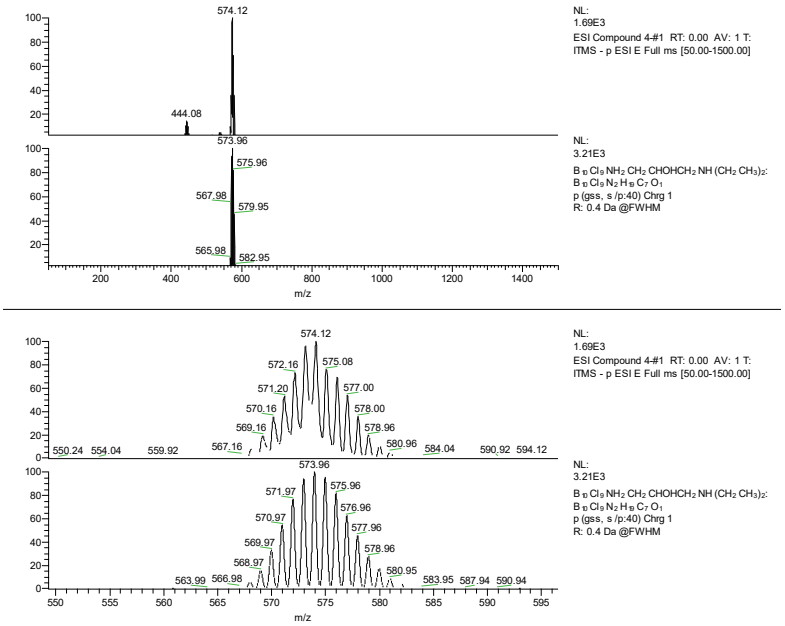

Fig. 35 Mass spectrum of **4**$^{-}$

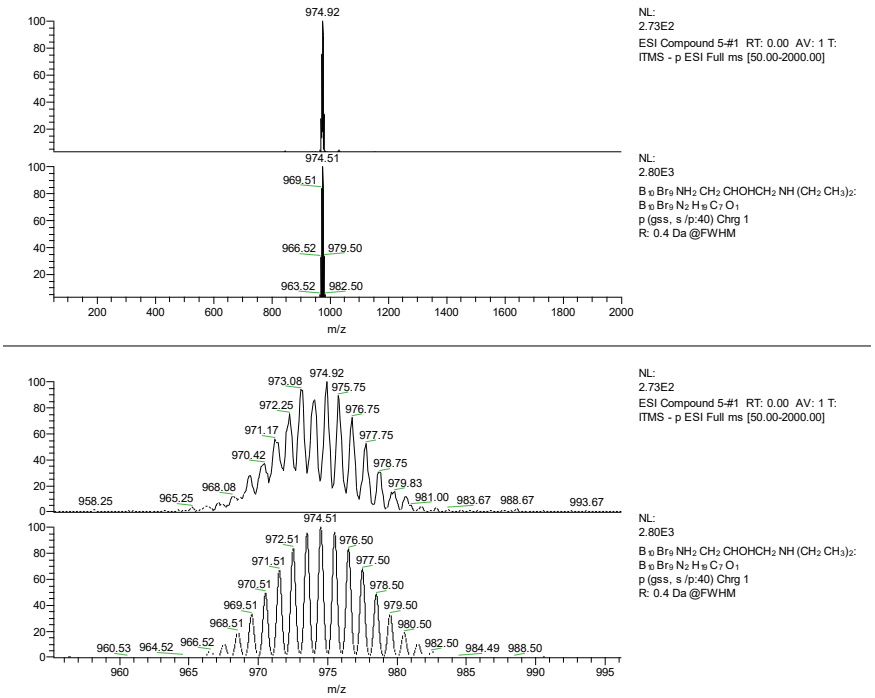

Fig. 36 Mass spectrum of **5**$^{-}$

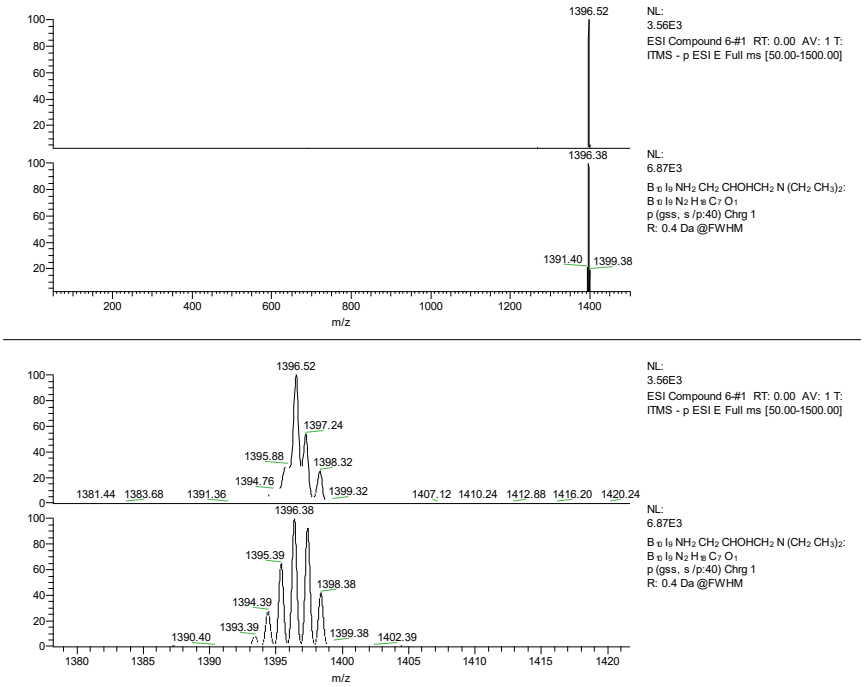

Fig. 37 Mass spectrum of **6**$^{-}$

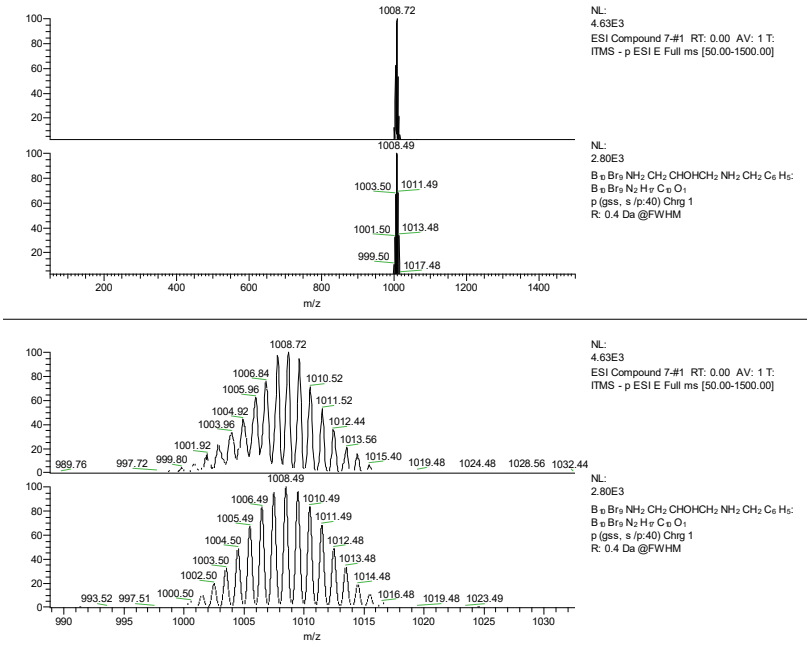

Fig. 38 Mass spectrum of **7**$^{-}$

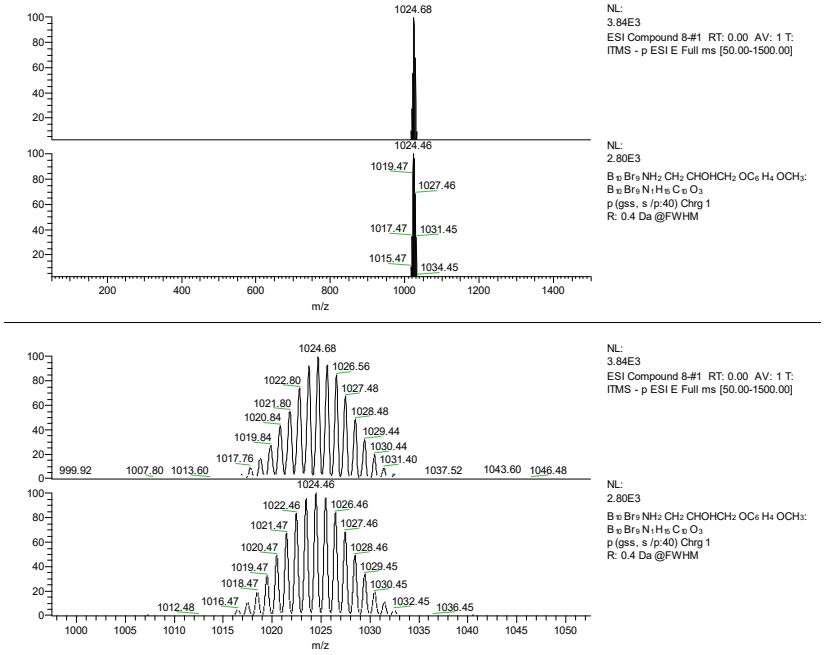

Fig. 39 Mass spectrum of **8**$^-$

References

1. J. Lubben, C. M. Wandtke, C. B. Hubschle, M. Ruf, G. M. Sheldrick and B. Dittrich, *Acta Crystallogr. Sect. A*, 2019, **75**, 50-62.
2. G. M. Sheldrick, *Acta Crystallogr. Sect. A*, 2015, **71**, 3-8.
3. S. El Anwar, J. Holub, O. Tok, T. Jelinek, Z. Ruzickova, L. Fojt, V. Solinova, V. Kasicka and B. Gruner, *J. Organomet. Chem.*, 2018, **865**, 189-199.
4. T. Peymann, E. Lork, M. Schmidt, H. Noth and D. Gabel, *Chem. Ber.-Recl.*, 1997, **130**, 795-799.
5. S. V. Ivanov, J. A. Davis, S. M. Miller, O. P. Anderson and S. H. Strauss, *Inorg. Chem.*, 2003, **42**, 4489-4491.
6. C. Bolli, J. Derendorf, C. Jenne, H. Scherer, C. P. Sindlinger and B. Wegener, *Chem.-Eur. J.*, 2014, **20**, 13783-13792.
7. Y. B. Zhang, J. Y. Liu and S. Duttwyler, *Eur. J. Inorg. Chem.*, 2015, 5158-5162.
8. M. Saleh, D. R. Powell and R. J. Wehmschulte, *Inorg. Chem.*, 2016, **55**, 10617-10627.